ISSN 2278-2540 | DOI: 10.51583/IJLTEMAS | Volume XV, Issue VI, June 2026

Geological Hazard Prediction and Prevention: A Review of Mechanisms, Monitoring, and Mitigation

Jeevana Sasindu Wickramaarachchige[1*], Daim Safeer Mughal[2]

[1]School of Environment and Civil Engineering, Chengdu University of Technology, Chengdu, China

[2]School of Management and Economics, Chongqing University of Post and Telecommunications, Chongqing, China

***Corresponding Author**

DOI: https://doi.org/10.51583/IJLTEMAS.2026.150600164

Received: 28 June 2026; Accepted: 03 July 2026; Published: 18 July 2026

ABSTRACT

As industrialization expands, modern infrastructure increasingly collides with volatile geological environments, driving a sharp escalation of complex, cascading geohazards. These destructive hazard chains represent a critical global threat to structural and economic resilience. Despite this escalating risk, current early warning systems predominantly rely on fragmented, static methodologies that fail to capture the dynamic reality of temporal hazard evolution. Furthermore, contemporary predictive models are bifurcated between deterministic physical models demanding exhaustive geotechnical parameters and data-driven artificial intelligence algorithms functioning as opaque black boxes devoid of physical interpretability. To resolve these limitations, this review systematically evaluates the modern geohazard landscape through a coupled active-passive conceptual model. This framework systematically evaluates how primary high-energy failures trigger subsequent instability in surrounding geomaterials. The synthesis reveals that integrating space-air-ground multi-scale monitoring including orbital InSAR, UAV photogrammetry, and distributed ground sensors establishes a vital surveillance continuum for early hazard identification. Because these heterogeneous data streams possess significant environmental noise, rigorous multi-source data fusion remains essential to minimize false alarms and resolve spatial discontinuities. Analytically, physically based models provide indispensable mechanical transparency by explicitly simulating material deformation, whereas data-driven ensemble algorithms excel at processing high-dimensional, nonlinear geospatial inputs. Ultimately, transitioning toward proactive, real-time risk reduction demands the integration of physics-informed neural networks (PINNs) that embed geomechanical constraints into computational pipelines. Coupling these hybrid architectures with interactive digital twin technologies will transform static hazard mapping into dynamic virtual environments, empowering engineers to successfully mitigate evolving disaster chains globally.

Keywords: Geological hazards; Disaster risk reduction; Real-time monitoring; Data-driven forecasting; Early warning systems; Physics-informed neural networks (PINNs).

INTRODUCTION

As industrialization and urban expansion push deeper into challenging terrains, the global footprint of infrastructure is colliding head-on with increasingly volatile geological environments. We are witnessing a sharp escalation in complex geohazards, ranging from earthquake-induced rockfalls along mountain corridors to catastrophic rockbursts in deep underground excavations. Consider the tragic events at the phosphate mine in Fuquan City, China, back in 2014. A massive rockfall and landslide plummeted into a deep pond, triggering a displacement wave of 50,000 cubic meters that resulted in 23 fatalities and extensive environmental devastation. Such disasters rarely operate in isolation. They frequently evolve into intricate geological-environmental hazard chains, where the initial mechanical failure triggers cascading secondary impacts like flooding or widespread soil and water contamination[1]. Confronting these cascading risks is no longer just a localized engineering

ISSN 2278-2540 | DOI: 10.51583/IJLTEMAS | Volume XV, Issue VI, June 2026

challenge; it is a critical global imperative for safeguarding human life, ecological stability, and economic resilience.

In an ideal scenario, hazard management would rely on dynamic, real-time early warning systems capable of seamlessly integrating subsurface mechanics with continuous monitoring data to predict the precise time, location, and magnitude of impending failures. Infrastructure planners would have access to high-fidelity, spatiotemporal forecasting that proactively identifies risk well before a steep slope gives way or a tunnel collapses. Yet, the reality on the ground falls drastically short of this vision. Current early warning systems and risk assessments predominantly rely on fragmented, reactive, or highly static methodologies. For example, traditional regional susceptibility maps typically reflect the spatial probability of failure under a specific seismic or rainfall scenario, but they utterly fail to account for temporal thresholds, progressive rock weakening, or site-specific energy accumulation[2]. We are mapping where disasters might happen based on static variables, but we are consistently missing the dynamic reality of exactly when and how they will unfold.

Previous attempts to solve this forecasting dilemma have largely bifurcated into two distinct camps: physical process-based models and data-driven algorithms. Physical approaches, such as the widely utilized Newmark displacement model, offer excellent mechanical interpretability by calculating critical acceleration and permanent displacement to assess slope stability[3,4]. Unfortunately, these deterministic models demand precise, comprehensive geotechnical parameters such as transient pore water pressure and shear strength, which are notoriously difficult and expensive to acquire across broad, heterogeneous regional scales[3,5]. Furthermore, they often rely on simplified assumptions, treating sliding masses as rigid bodies while neglecting complex internal deformations and dynamic topographic amplification effects[6]. Conversely, the recent surge in deep learning and machine learning models provides a highly scalable alternative capable of processing vast amounts of remote sensing data[3]. Even so, these artificial intelligence approaches function predominantly as black boxes. They learn statistical correlations rather than physical mechanisms, which makes them highly susceptible to domain shifts, meaning a model trained on one geological setting frequently fails when applied to another with different lithology or climate conditions[7]. Moreover, optimizing these algorithms solely to maximize statistical hit rates often generates unacceptable levels of false alarms, ultimately undermining the social credibility of the early warning systems they are meant to support[6].

The direct and indirect consequences of relying on these inadequate, decoupled systems are severe. Directly, unforeseen landslides and deep-tunnel rockbursts lead to catastrophic loss of life and the sudden destruction of critical transportation networks and energy grids[8,9]. Indirectly, the fallout is even more insidious. When a major transportation artery is severed by a rockfall, the ensuing highway blockages paralyze regional trade, disrupt emergency response efforts, and trigger prolonged economic stagnation in communities that lack viable alternate routes[10]. Beyond the economic toll, misclassifying or entirely missing the precursory signals of a major slope failure can lead to environmental disasters that persist for decades, as seen when mining slopes collapse and release toxic materials into local watersheds[1,11].

What remains glaringly absent from the current literature is a cohesive framework that bridges the gap between macroscopic data-driven forecasting and microscopic, physics-based failure mechanisms. For instance, while recent work has successfully integrated multi-geometry InSAR with explainable machine learning to map potential landslide areas in reservoir regions, these frameworks still treat susceptibility as a relatively static baseline rather than a time-resolved, dynamic state[12]. Similarly, advancements in microseismic monitoring have revolutionized our ability to track deep rock microfractures in real-time[6], yet integrating these high-frequency, localized signals into broader regional vulnerability models remains a significant hurdle[13]. This study seeks to fill that exact void by examining the hazard landscape through the lens of a coupled active-passive conceptual model. In this framework, primary high-energy brittle failures (the active source) trigger the subsequent instability of surrounding fractured rock masses (the passive response), a dynamic particularly evident in compound rockburst-collapse events[14]. By adopting this theoretical lens, we can better decode how localized stress concentrations dynamically interact with external triggers like extreme rainfall or seismic shocks.

Accordingly, the primary objective of this review is to systematically evaluate the underlying mechanisms of complex geological hazards, critically assess the efficacy and limitations of emerging multi-source monitoring

ISSN 2278-2540 | DOI: 10.51583/IJLTEMAS | Volume XV, Issue VI, June 2026

technologies, and test the theoretical boundaries of both physical and AI-driven forecasting models. Specifically, we aim to investigate how the integration of ground-based sensor networks, such as distributed fiber optic sensing, with intelligent predictive algorithms can successfully transition hazard management from reactive post-disaster analysis to proactive, real-time early warning[15]. In practical terms, this research is vital for engineers and policymakers who require robust, uncertainty-aware decision-support tools that function reliably under the chaotic, non-stationary conditions of real-world environments[6]. Academically, it establishes a necessary dialogue between geomechanics and artificial intelligence, charting a realistic course toward physically-informed foundation models.

Ultimately, managing geological hazards is paramount for ensuring the resilience and sustainability of our expanding global infrastructure. Despite an abundance of sophisticated monitoring tools and advanced computational algorithms, current research remains highly fragmented, leaving a critical gap in our ability to synthesize real-time dynamic monitoring with transparent, physically grounded predictive models. This paper occupies that exact niche by offering a comprehensive review. The subsequent sections are logically organized to unravel this complexity: first, we dissect the intricate failure mechanisms driving modern geohazards; next, evaluate the state-of-the-art in remote and ground-based monitoring systems; finally, critically analyze current forecasting models, outlining a strategic roadmap for the future of intelligent, multi-hazard disaster risk reduction.

Formation Mechanisms of Geological Hazards

Internal Geological Factors

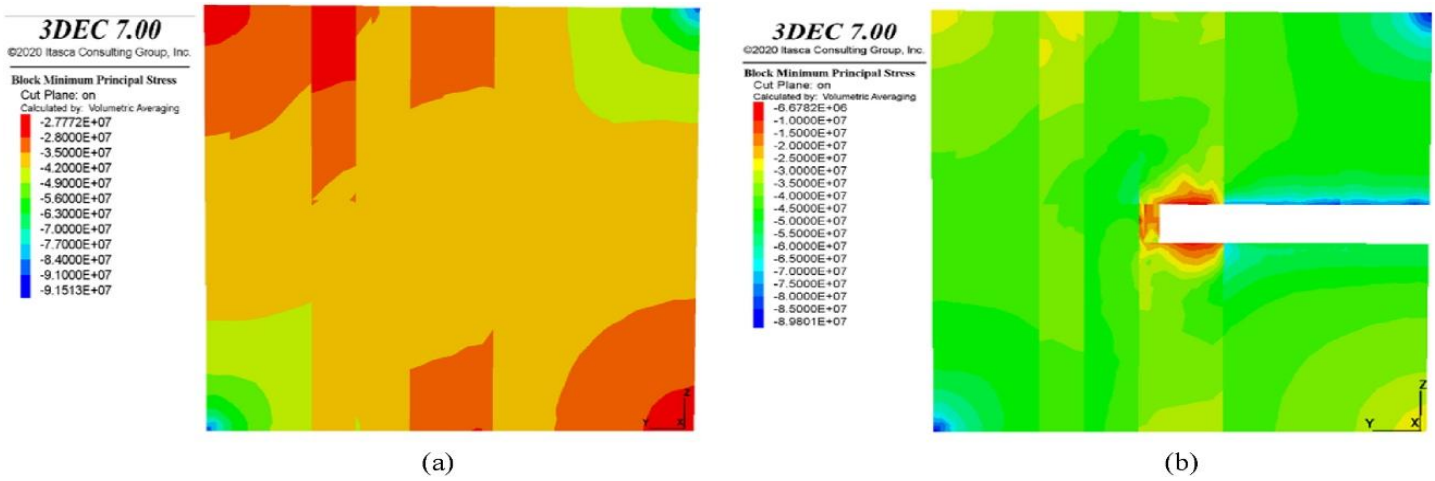
The geometric boundary conditions of a landscape establish the fundamental gravitational framework for slope instability. Terrain steepness directly dictates the magnitude of shear stress acting parallel to potential failure surfaces. This means steeper gradients inherently elevate the probability of mass displacement[8]. This geometric influence is further modulated by slope aspect. Aspect controls local microclimates by determining solar radiation and moisture retention[16,17]. Such variations alter vegetation density and chemical weathering rates, which indirectly shape the mechanical resistance of surficial materials[18]. Beyond simple inclination and orientation, hillside curvature determines the pathways of surface runoff and the accumulation of loose colluvium[8,17]. Concave topographic hollows serve as natural convergence zones for groundwater. They facilitate rapid increases in pore pressure during precipitation events that frequently initiate shallow landsliding[16,19]. Beneath this topographic surface, regional tectonic activity deeply compromises terrain stability through the formation of complex fault zones[20,21]. Major geological faults and their associated damage corridors shatter intact bedrock. They produce thick bands of low-strength fault gouge and highly permeable fragmented materials[12,14,18]. These structural discontinuities not only reduce the overall compressive and shear capabilities of the rock mass, but they also create preferential infiltration channels that accelerate deep fluid migration[22,23]. When slopes are situated within these tectonically active corridors, the combination of mechanically degraded lithology and heightened groundwater accumulation dramatically increases the propensity for large-scale failure[18,20]. Operating at a more localized scale, intrinsic rock mass properties and secondary discontinuities define the specific kinematic mechanisms of failure[18]. The stability of a bedrock slope is largely governed by its lithological composition alongside the orientation of its internal structural planes, such as bedding, foliation, and joints[24,25]. Intact, massive rocks like granodiorite typically resist weathering and exhibit high geomechanical strength[25]. In contrast, heterogeneous formations containing alternating hard and soft strata weather unevenly. Interbedded sandstone and mudstone, for instance, rapidly form discrete, low-strength slip surfaces[5,24,26]. The spatial alignment of these planes relative to the slope face determines the physical mode of collapse[18]. Planar sliding readily occurs when discontinuities strike parallel to the slope and dip at angles exceeding the internal friction angle but less than the slope face. Alternatively, intersecting joint sets can isolate individual tetrahedral wedges that detach under gravitational pull. Steeply dipping vertical fractures often promote toppling mechanisms instead[25]. Over geological time, intensive weathering degrades these rock masses into compressible residual soils. This shifts the governing failure mechanics from structural detachment to hydro-mechanical soil yielding. Within these soil mantles, stability depends entirely on a delicate physical balance. The shear strength, derived from cohesion and the effective angle of internal friction, must adequately resist the downslope driving forces[2,27]. As meteoric water infiltrates the porous matrix, it steadily

ISSN 2278-2540 | DOI: 10.51583/IJLTEMAS | Volume XV, Issue VI, June 2026

dissipates matric suction and elevates positive pore water pressure. This fundamentally diminishes the effective stress holding the soil particles together[19,28,29]. For highly compressible residual soils, rapid shearing can induce localized pore pressure spikes and severe strain softening, ultimately driving the material into a state of residual strength[30]. Once this localized yielding initiates near the over-steepened toe of a slope, the loss of lateral support transfers stress upslope. A retrogressive cascade of progressive soil failure then inevitably follows[31,32].

External Triggering Factors

Geohazards rarely initiate without external forcing mechanisms that disrupt the mechanical equilibrium of slopes. Precipitation acts as the most ubiquitous catalyst for mass wasting globally[31]. When meteoric water infiltrates the subsurface, it progressively fills pore spaces, which simultaneously dissipates matric suction and elevates positive pore water pressure[33–35]. This hydrodynamic alteration fundamentally diminishes the effective stress and shear resistance of the geomaterials while adding significant gravitational mass to the potential sliding body[18,33,36]. The temporal distribution of this precipitation dictates the specific failure mechanics. Short-duration, high-intensity rainstorms typically induce rapid shallow landsliding, whereas prolonged antecedent moisture accumulation governs the activation of deep-seated structural failures[18]. In high-altitude or frigid mountain catchments, these hydrological effects are further compounded by seasonal snowmelt and thermal fluctuations[18,37]. Rapid spring warming accelerates cryospheric melt, delivering substantial fluid pulses that infiltrate fractured bedrock and residual soils[20,37]. Antecedent freeze-thaw cycles physically degrade the rock mass by expanding existing fissures during freezing periods[20,38]. This repeated expansion and contraction ultimately leaves the slope highly susceptible to hydro-mechanical yielding once thawing occurs[18,36]. Beyond hydrological drivers, tectonic disturbances represent a dominant dynamic trigger, particularly in active orogenic belts. Earthquakes subject slope materials to sudden, intense inertial and shear forces that frequently exceed the available frictional resistance of internal discontinuities[3,10,39]. Seismic shaking causes instantaneous co-seismic fracturing and potential soil liquefaction[18,40,41]. This shaking is also subject to significant topographic amplification along steep ridges and cliff edges[10,41,42]. Amplified kinetic energy drives the rapid detachment of unstable rock blocks and can generate catastrophic, long-runout mass movements[10]. Furthermore, the structural degradation inflicted by seismic wave propagation leaves the landscape preconditioned for subsequent rainfall-induced secondary hazards, initiating complex disaster chains[41,43]. Human engineering interventions have increasingly become primary instigators of slope instability, mirroring the destructive potential of natural triggers. Subsurface mining operations fundamentally disrupt the primordial geostress field[15,44]. The extraction of underground orebodies or coal seams induces a massive redistribution of stress, leading to the progressive deformation, tension cracking, and eventual subsidence or catastrophic collapse of the overlying strata[44–46]. To visualize this mechanical disruption, Figure 1 illustrates the severe concentration and redistribution of principal stress localized around an advancing underground excavation face compared to the undisturbed geostress field.



(a) (b)

Figure 1: Principal stress distribution before and after underground excavation. The initial geostatic equilibrium (a) is fundamentally disrupted by the advancing face (b), triggering massive, localized stress redistribution[14].

ISSN 2278-2540 | DOI: 10.51583/IJLTEMAS | Volume XV, Issue VI, June 2026

Conversely, open-pit mining, road construction, and agricultural terracing directly modify the terrain geometry[15,47]. These activities often involve aggressive slope cutting that removes essential basal support and creates over-steepened, artificial free faces. Similarly, the construction and operation of major hydropower reservoirs impose severe hydro-mechanical stressors on valley flanks[34,48]. The periodic fluctuation of reservoir water levels subjects the submerged rock and soil to cyclic wetting and drying, which progressively softens the materials and degrades their overall shear strength[5,12]. During phases of rapid water drawdown, the delayed dissipation of internal groundwater creates steep hydraulic gradients[18]. This phenomenon generates powerful outward-directed seepage forces that compromise the stability of the reservoir banks, frequently reactivating dormant ancient landslides or triggering sudden rockfalls[5,18,24].

Coupling Effects

Geological hazards rarely emerge from isolated triggers; rather, they manifest through the complex, non-linear interaction of multiple physical fields. The transition from a stable state to catastrophic failure is fundamentally governed by hydro-mechanical coupling, particularly during severe precipitation events[3,49]. As rainwater permeates the subsurface, it initiates a sequence of interacting physical alterations within the rock and soil mass. Initially, infiltration diminishes matric suction and elevates pore water pressure, which directly reduces the effective stress and frictional resistance along potential slip surfaces[33,50,51]. Concurrently, the accumulated fluid adds significant gravitational mass to the slope, increasing the driving downward forces[33,40]. This hydrodynamic alteration degrades the structural integrity of the geomaterials, often softening clay-rich or heavily weathered strata[36]. Beyond uniform saturation, transient groundwater flow generates powerful seepage forces that can erode fine particles within the matrix, thereby creating localized preferential flow networks[31,34]. In highly permeable residual soils, this process can trigger a distinct physical cascade where rapid internal erosion and localized pore pressure spikes overcome the remaining shear strength, driving the material into an unstable state[18,34].

This hydrological mechanism is frequently exacerbated by static and dynamic stresses in anthropogenically modified terrains, initiating a synergistic tri-field coupling effect of cracks, external loads, and rainfall. Excavations for transportation networks or residential infrastructure impose static stress redistributions that often generate initial tension cracks along the slope crest or toe. These structural discontinuities dramatically alter the infiltration geometry by providing direct, low-resistance channels for preferential water flow. When subjected to cyclic dynamic loading from passing traffic or heavy machinery, the rock-soil mass experiences progressive material fatigue, causing these initial mechanical fractures to propagate further into the subsurface. The synergistic amplification between mechanical crack growth and hydraulic fracturing dictates that even short-duration rainstorms can induce instantaneous pore pressure surges deep within the slope, bypassing the slower matrix infiltration process entirely and leading to sudden block detachment[51].

Similar coupled dynamics govern slope behavior during seismic events, where transient ground shaking interacts violently with subsurface hydrology. Earthquakes subject slopes to intense inertial forces while simultaneously altering internal fluid pressures. In fractured or partially saturated geological formations, seismic waves can compress pore spaces, leading to sudden, localized spikes in pore water pressure that drastically reduce inter-particle cohesion[10]. Even if a hillside survives the immediate shaking, co-seismic fracturing permanently lowers the overall geomechanical stability threshold[23]. These newly formed structural weaknesses precondition the terrain, allowing subsequent rainfall to infiltrate deeply and trigger delayed, post-seismic mass movements[52]. Ultimately, the synchronized action of these coupled forces dictates not only the initiation of a hazard but also its evolutionary trajectory. Once a sliding mass detaches, the combined effects of high moisture content and accumulated kinetic energy can induce rapid fluidization[1]. The mobilized debris then aggressively scours the channel bed and banks, incorporating additional loose alluvium and amplifying its destructive volume as it accelerates downslope[1,53]. The synchronized action of these coupled forces dictates not only the initiation of a hazard but also its evolutionary trajectory. To visually synthesize these interacting physical fields, Figure 2 illustrates a conceptual cross-section of hydro-mechanical coupling, demonstrating how surface rainfall infiltration, internal pore pressure accumulation, and anthropogenic toe excavation synergistically drive slope instability.

ISSN 2278-2540 | DOI: 10.51583/IJLTEMAS | Volume XV, Issue VI, June 2026

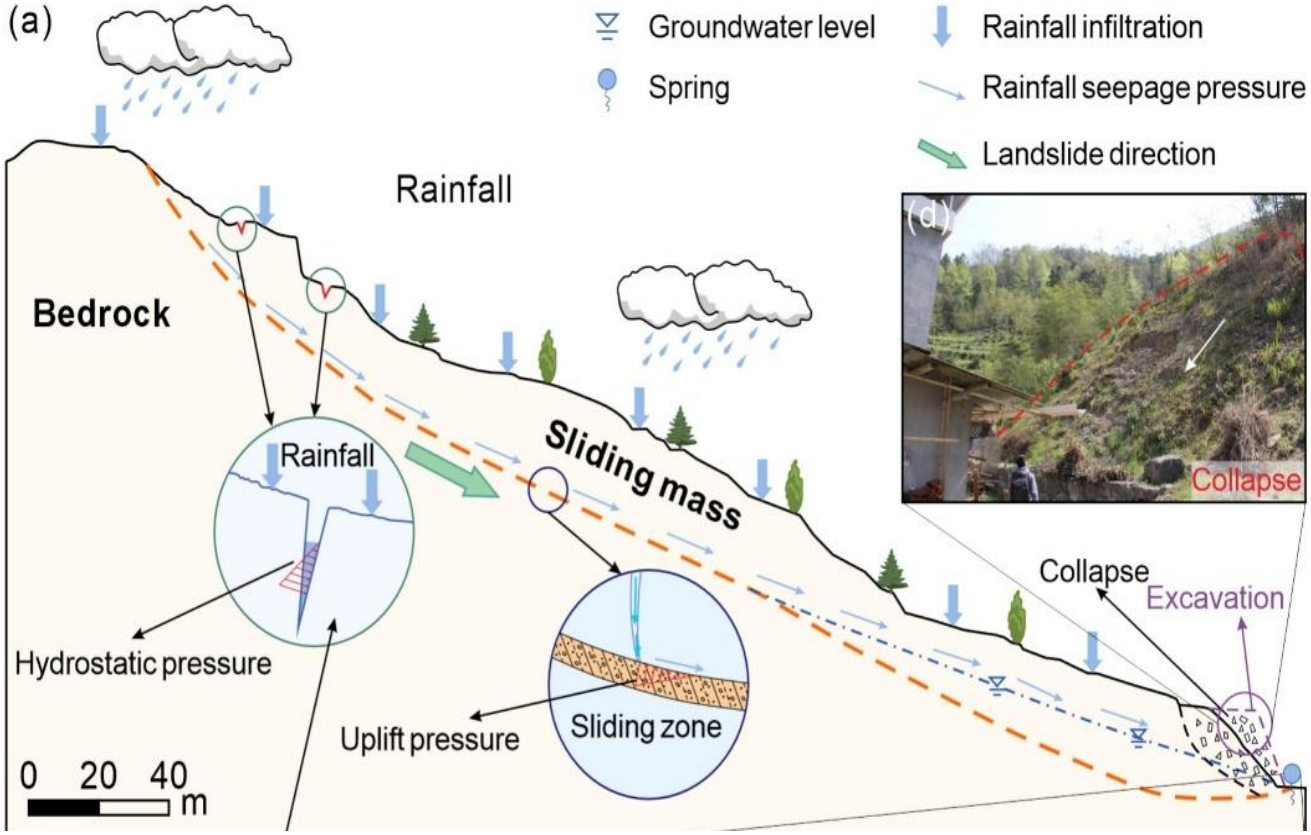


Figure 2: Conceptual model of hydro-mechanical coupling in slope instability[34]

Early Identification of Hidden Hazards

Satellite Remote Sensing

Interferometric synthetic aperture radar fundamentally operates by calculating phase shifts between successive microwave pulses to map surface displacement at the millimeter scale[7,54]. Within this technological domain, the Small Baseline Subset algorithm specifically minimizes both atmospheric phase delays and spatial-temporal decorrelation by establishing strict thresholds for interferometric pairing[12,55,56]. Consequently, this approach maintains phase stability across highly vegetated slopes and topographically varied environments, thereby outperforming permanent scatterer techniques that demand dense, stable targets[56]. Single-orbit radar acquisitions inherently constrain deformation data to a one-dimensional line-of-sight vector, frequently underrepresenting the magnitude of actual ground movement and struggling to detect north-south kinematic shifts[12,55]. Fusing independent ascending and descending flight paths resolves this geometric ambiguity. Decomposing these intersecting lines of sight allows geoscientists to reconstruct complete two-dimensional and three-dimensional deformation velocity fields, which more accurately reflect the true translational or rotational failure mechanisms of a given slope[12,52]. Radar monitoring still encounters significant environmental constraints. Steep terrain produces complex geometric distortions, primarily layover and shadowing effects, that physically obscure the radar signal in deeply incised valleys[7,55,57]. Moreover, sudden displacement accelerations immediately preceding a collapse, alongside dense forest canopies induce abrupt phase decorrelation, causing temporary observation gaps during critical pre-failure windows[7,57,58]. High-resolution optical sensors complement these radar deficiencies by capturing precise surface morphology and multi-spectral reflectance[18,59,60]. Data from platforms like Sentinel-2 and the Gaofen constellation provide the sub-meter optical clarity necessary to visually trace tension cracks, map active scarp retreat, and verify land-cover alterations following a displacement event[37,59,60]. Passive optical imaging is nonetheless severely limited by its dependence on clear atmospheric conditions. Heavy cloud cover during intense monsoon rainfall, which is the exact periods when landslide probability maximizes, renders optical satellites essentially blind[6,15]. Fusing these contrasting modalities establishes a comprehensive monitoring continuum[60]. Integrating the continuous, cloud-penetrating kinematic measurements of radar with the discrete, high-fidelity spatial boundaries of optical

ISSN 2278-2540 | DOI: 10.51583/IJLTEMAS | Volume XV, Issue VI, June 2026

imagery allows analysts to confirm the geological origin of a moving mass[12]. This integrated methodology successfully differentiates deep-seated slope instability from shallow anthropogenic ground disturbances, substantially minimizing the occurrence of false-positive hazard classifications[12,24].

UAV and Ground-Based Surveys

Unmanned aerial vehicles routinely acquire overlapping high-resolution imagery along pre-programmed flight trajectories, relying on structure-from-motion and aerial triangulation algorithms to reconstruct complex terrain geometries into dense three-dimensional point clouds, digital surface models, and orthomosaics[37,61]. To ensure precise georeferencing in environments where deploying ground control points is physically hazardous, modern aerial platforms integrate real-time or post-processed kinematic global navigation satellite systems[19,40]. This positional accuracy enables analysts to apply digital image correlation and optical flow techniques directly to the sequential aerial datasets, extracting sub-pixel displacement vectors and tracking the progressive deformation of open-pit slopes or landslide scars[36,39]. The acquisition of multi-angle oblique photographs further facilitates the extraction of structural data and the construction of high-fidelity digital twins for immersive virtual reality assessments of active mining operations[36,62]. Aerial photogrammetry nonetheless suffers from inherent limitations in forested topographies, as passive optical sensors cannot resolve bare-earth features beneath dense vegetative canopies[9,39,63]. Light detection and ranging systems overcome this observational barrier by emitting high-frequency laser pulses and measuring the time of flight of the returning backscatter[9]. Because multiple return signals can be isolated from a single emitted pulse, LiDAR effectively penetrates foliage gaps to generate accurate digital terrain models of the underlying bedrock and geomorphic depressions[9,40]. When mounted on automated aerial platforms, these active sensors rapidly survey vast, inaccessible orogenic belts and fault zones, capturing the structural architecture of the landscape without exposing field personnel to imminent collapse risks[9]. Operating at the ground level, terrestrial and dynamic laser scanning systems supplement these airborne campaigns by delivering millimeter-scale resolution across near-vertical rock faces and deeply incised gorges[15]. Terrestrial scanners project discrete laser beams against exposed outcrops, extracting the orientation, persistence, and spacing of rock mass discontinuities that dictate the kinematic feasibility of wedge failures or toppling events. Fusing the multi-spectral textural fidelity of photogrammetry with the structural penetration of LiDAR establishes a comprehensive surveying continuum[40]. By co-registering these multi-source point clouds over successive monitoring campaigns, geoscientists compute high-resolution digital elevation models of difference[8]. This subtraction process directly quantifies volumetric material loss from detachment zones, measures the accumulation of debris along runout pathways, and isolates subtle micro-topographic anomalies such as incipient tension cracks or localized subsidence that frequently precede catastrophic mass movements[8,15,37].

Machine Learning for Hazard Detection

Convolutional neural networks automatically extract hierarchical spatial features directly from multi-spectral and radar imagery, circumventing the need for manual feature engineering[3,6,64]. By applying successive convolutional and pooling layers, these architectures identify low-level edges and high-level morphological patterns indicative of slope failure[6]. Within this domain, computer vision applications generally bifurcate into object detection and semantic segmentation[24]. Object detection algorithms, including Faster R-CNN and YOLO variants, localize active deformation zones and historical scars by generating bounding boxes around suspected geohazards[24,65]. While these models offer rapid localization, bounding boxes inherently fail to capture the irregular physical boundaries of mass movements. Semantic segmentation resolves this geometric limitation by classifying input imagery strictly at the pixel level[24,64]. Architectures such as U-Net employ a symmetric encoder-decoder structure where skip connections transfer low-level spatial details directly across the network. This mechanism preserves the fine-grained edge resolution necessary to delineate complex landslide scarps from stable terrain[57]. Other specialized segmentation frameworks, such as fully convolutional networks and image cascade networks, process varying resolutions to capture both broad spatial patterns and localized geomorphic anomalies simultaneously. To further improve discrimination in visually complex environments, multi-modal architectures like the RGB-D fusion network integrate optical spectral reflectance with digital elevation depth data. Processing these distinct data streams through recursive dilated convolutions allows the network to isolate specific topographic cues, such as steep failure flanks or accumulated debris flows, that purely spectral models

ISSN 2278-2540 | DOI: 10.51583/IJLTEMAS | Volume XV, Issue VI, June 2026

frequently overlook[64]. Identifying historical hazard scars triggered by specific extreme events relies heavily on multi-feature change detection algorithms applied to pre- and post-event satellite optical imagery. These methods often utilize principal component analysis and independent component analysis to highlight structural deviations while suppressing background environmental noise[6]. Recent structural modifications to these visual processing models increasingly incorporate attention mechanisms and Vision Transformers[6,7]. These transformer blocks capture long-range spatial dependencies across an image that traditional, highly localized convolution kernels might miss[7]. Hybrid models subsequently fuse these transformer outputs with morphological edge detection techniques to smooth the jagged discretization frequently observed during automated boundary extraction. A persistent constraint in training these deep learning models is the severe scarcity of high-quality, manually annotated hazard inventories. To mitigate class imbalance and limited sample sizes, generative adversarial networks are deployed to synthesize realistic image patches, effectively expanding the available training data without requiring additional physical field surveys. Transfer learning strategies address this exact computational bottleneck by initializing networks with weights pre-trained on massive, generalized global datasets before fine-tuning them on localized target imagery. This targeted knowledge transfer significantly reduces the requirement for extensive local sampling while maintaining high detection accuracy across highly diverse geological domains[6].

Monitoring And Early Warning Systems

Sensor Networks and IoT Integration

Modern geological monitoring systems increasingly rely on the Internet of Things to connect distributed sensor arrays directly to cloud-based analytical platforms, thereby eliminating the physical vulnerabilities and high deployment costs associated with traditional wired instrumentation[66,67]. Within this architecture, wireless sensor networks transmit high-frequency environmental and mechanical data across challenging topographies using low-power, long-range communication protocols such as LoRaWAN or 4G cellular networks[50,67]. To capture macroscopic surface displacements, global navigation satellite system receivers continuously track three-dimensional coordinate variations.

By employing real-time kinematic positioning, these receivers achieve millimeter-level accuracy and bypass cumulative errors, although their operational efficacy remains sensitive to signal obstruction in deep canyons or beneath dense forest canopies[15]. Complementing this regional spatial data, localized surface fracturing is monitored using high-sensitivity crack meters and wireline extensometers. These instruments translate the minute opening of tension fissures into digital electrical or optical signals, delivering instantaneous alerts when surface displacement rates suddenly accelerate[15,36].

Because surface sensors cannot map the internal structural degradation of a sliding mass, subsurface deformation must be tracked using embedded inclinometers and tiltmeters. Deep borehole inclinometers capture lateral subsurface movement along the vertical profile to accurately locate deep-seated shear zones[15]. Similarly, advanced micro-electro-mechanical systems measure the gravitational tilt of specific strata, continuously recording the angular variations that indicate progressive slope yielding[25]. Because slope instability is fundamentally governed by subsurface hydrology, mechanical tracking is systematically coupled with groundwater instrumentation[28]. Piezometers and tensiometers are deployed at varying depths to measure transient pore water pressures and soil matric suction[33,68].

When integrated within a unified wireless network, these distributed piezometric readings allow geoscientists to observe exactly how rainfall infiltration progressively dissipates effective stress within the soil matrix[18,25]. The real-time synchronization of these diverse field instruments successfully transitions hazard assessment from a sequence of periodic manual surveys into an automated, data-driven surveillance continuum[50,69]. To contextualize the physical architecture supporting this network, Table 1 synthesizes the primary operational capabilities and environmental limitations of the remote sensing and ground-based monitoring technologies discussed thus far.

ISSN 2278-2540 | DOI: 10.51583/IJLTEMAS | Volume XV, Issue VI, June 2026

Table 1: Operational comparison of remote sensing and ground-based monitoring technologies for geological hazard assessment

Technology Category	Specific Methods	Primary Application	Key Strengths	Fundamental Limitations	Source
Satellite Radar	SBAS-InSAR, PS-InSAR, D-InSAR	Regional tracking of subsidence basins and slow-moving landslides.	All-weather operational capacity, extensive spatial coverage, and millimeter-level kinematic precision.	Susceptible to vegetation decorrelation, atmospheric phase delays, and restricted by fixed satellite revisit cycles.	[12,15,60]
Satellite Optical	Multispectral, hyperspectral, and Thermal Infrared (TIR).	Macroscopic land cover mapping, ecological assessment, and surface thermal anomaly detection.	Cost-effective regional surveillance with rich spectral discrimination and nocturnal observation capabilities.	Highly vulnerable to cloud cover, fog, and dust; incapable of penetrating dense vegetation canopies.	[15,59]
Aerial Surveying	UAV photogrammetry, Airborne LiDAR, and Structure-from-Motion (SfM).	Generating high-resolution 3D digital elevation models and localized morphological crack mapping.	Highly flexible rapid deployment, sub-centimeter spatial resolution, and effective vegetation penetration via LiDAR.	Flight operations are restricted by adverse meteorological conditions, limited battery endurance, and heavy data processing demands.	[15,40]
Surface Sensors	GNSS, tiltmeters, and fissure/crack meters.	Monitoring localized fracture propagation and instantaneous surface coordinate variations.	Delivers continuous, real-time data transmission with high sensitivity for immediate macroscopic failure warning.	Sparse point-based spatial density, susceptibility to signal multipath interference, and physical vulnerability to environmental damage.	[15,25]
Subsurface Sensors	Deep borehole inclinometers, piezometers, and microseismic arrays.	Isolating deep shear zones, tracking transient pore pressures, and localizing micro-fracture acoustic emissions.	Directly captures internal hydro-mechanical yielding and precursory stress changes prior to surface deformation.	Requires highly invasive borehole excavation, prone to sensor shearing from structural collapse, and experiences signal attenuation.	[15,25,70]

Data Fusion and Processing

Raw monitoring streams inherently contain environmental interference and measurement anomalies that necessitate aggressive preprocessing before analytical integration. Statistical methods like the Pauta criterion establish dynamic confidence intervals based on standard deviations to isolate and discard transient outliers triggered by extreme weather or localized construction vibrations[62]. For high-frequency acoustic and microseismic data, spectral subtraction algorithms decompose original signals into amplitude and phase spectra, subtracting stationary background noise before reconstructing the clean waveforms[70]. Similarly, adaptive time-frequency transformations, such as db4 wavelet denoising or orthogonal master-slave adaptive notch filters, systematically eliminate periodic noise components while preserving the physical characteristics of early fracture signatures[13,71]. Once individual sensor streams are purified, the analytical focus shifts to resolving the spatial and semantic discontinuities between heterogeneous observation platforms. Integrating meteorological radar,

ISSN 2278-2540 | DOI: 10.51583/IJLTEMAS | Volume XV, Issue VI, June 2026

ground-based piezometers, and unmanned aerial vehicle topography establishes the necessary boundary conditions for dynamic hydro-mechanical modeling[37]. Figure 3 visualizes this integrated space-air-ground monitoring architecture, illustrating how these diverse sensor streams converge into a centralized data fusion center.

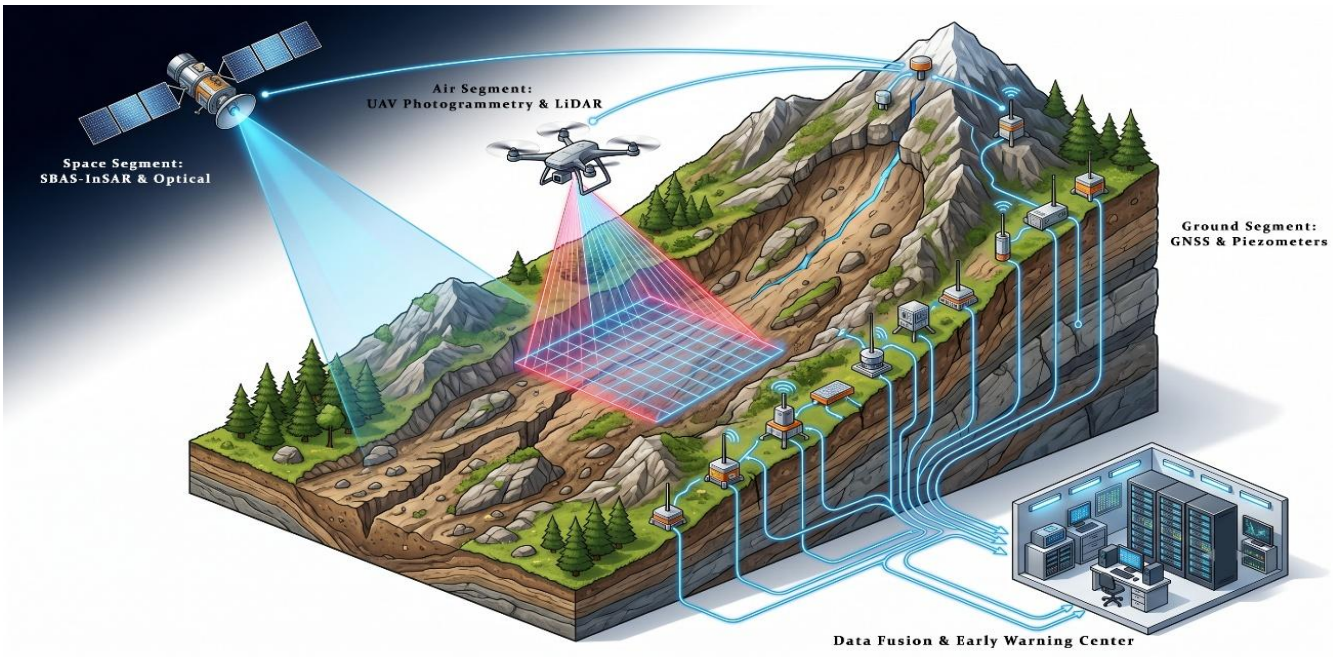


Figure 3: Architecture of an integrated space-air-ground multi-scale geological hazard monitoring system

Aligning these ground-level metrics with orbital remote sensing demands specialized cross-modal architectures. To harmonize optical imagery, which excels at delineating surface morphology but is easily obscured by cloud cover, with all-weather synthetic aperture radar, deep learning frameworks frequently utilize domain-sharing encoders. These architectures project disparate spectral and microwave signals into a unified feature space, applying pointwise convolutions and attention mechanisms to suppress modality-specific biases[60]. The subsequent fusion of these aligned spatial features with temporal meteorological inputs introduces significant predictive uncertainty. Researchers increasingly apply Dempster-Shafer evidence theory to calculate the joint probability of multi-source warning indicators to mitigate this ambiguity. This probabilistic formulation treats conflicting sensor readings as probability masses, dynamically reallocating support to resolve contradictions between localized crack gauge accelerations and stable regional radar interferograms[62,72]. Complementing this probabilistic reasoning, multi-model ensemble strategies concurrently process the fused data arrays. Hybrid temporal networks deploy parallel architectures such as Long Short-Term Memory units, Gated Recurrent Units, and frequency-aware Transformers to extract long-range dependencies from the homogenized time-series data. By optimizing the predictive weights of each base learner through genetic algorithms or empirical risk functions, these ensemble matrices effectively stabilize the variance inherent in multi-sensor environments and generate continuous, physically coherent risk trajectories[73].

Early Warning Thresholds

Establishing actionable warning triggers requires translating raw environmental and kinematic data into defined boundaries that signify impending slope failure. In meteorological monitoring, empirical power-law relationships frequently define the minimum forcing required to initiate instability by plotting accumulated rainfall against event duration. To optimize these boundaries for public alert systems, analysts employ frequentist approaches that set specific non-exceedance probabilities, deliberately balancing true positive predictions while minimizing false alarm rates[74]. Beyond single-variable duration limits, contemporary hazard management utilizes double-index models to capture complex hydrological interactions. These models evaluate short-term storm intensity, such as daily precipitation, alongside antecedent moisture accumulation spanning five to fifteen days[47,63]. By cross-referencing immediate rainfall with prior effective infiltration, these systems establish

ISSN 2278-2540 | DOI: 10.51583/IJLTEMAS | Volume XV, Issue VI, June 2026

graded alert tiers ranging from low advisories to very high emergency evacuation levels[47]. Physics-based models further modulate these meteorological limits by incorporating the initial saturation state of the soil profile. Field tests demonstrate that during dry seasonal conditions, the required cumulative rainfall to breach safety thresholds is significantly higher than during wet periods, reflecting the initial buffering capacity of unsaturated pore spaces[35].

When environmental forcing translates into physical ground movement, kinematic thresholds provide a direct measurement of the progression toward catastrophic collapse. A widely adopted standard for defining these critical failure points is the improved tangent angle method, which mathematically transforms displacement time-series curves into angular metrics. Within this evaluation system, angles below 45 degrees indicate primary, stable creep. Once the tangent angle reaches 45 degrees, the geomaterial enters a constant-rate secondary deformation stage, whereas angles exceeding 85 degrees typically trigger terminal red alerts denoting imminent tertiary failure. This angular metric is frequently combined with hard limits on cumulative displacement and daily deformation velocity to formulate a comprehensive instability index[62]. To isolate the exact temporal transition into the dangerous acceleration phase, statistical techniques compute the normal fluctuation range of a stable slope and identify the onset of acceleration point when deformation velocity permanently deviates from this baseline[75]. For macroscopic regional surveillance utilizing satellite interferometry, distinct kinematic thresholds isolate hazardous slopes from stable terrain. Researchers have proposed that slopes exhibiting settlement rates exceeding 30 millimeters per year, or cumulative displacements beyond 80 millimeters, should be automatically flagged as potential landslide points demanding immediate intervention[57]. To visualize this kinematic progression and the corresponding stability thresholds, Figure 4 illustrates the standard three-stage creep deformation curve, highlighting the critical temporal transitions from steady-state creep to terminal acceleration.

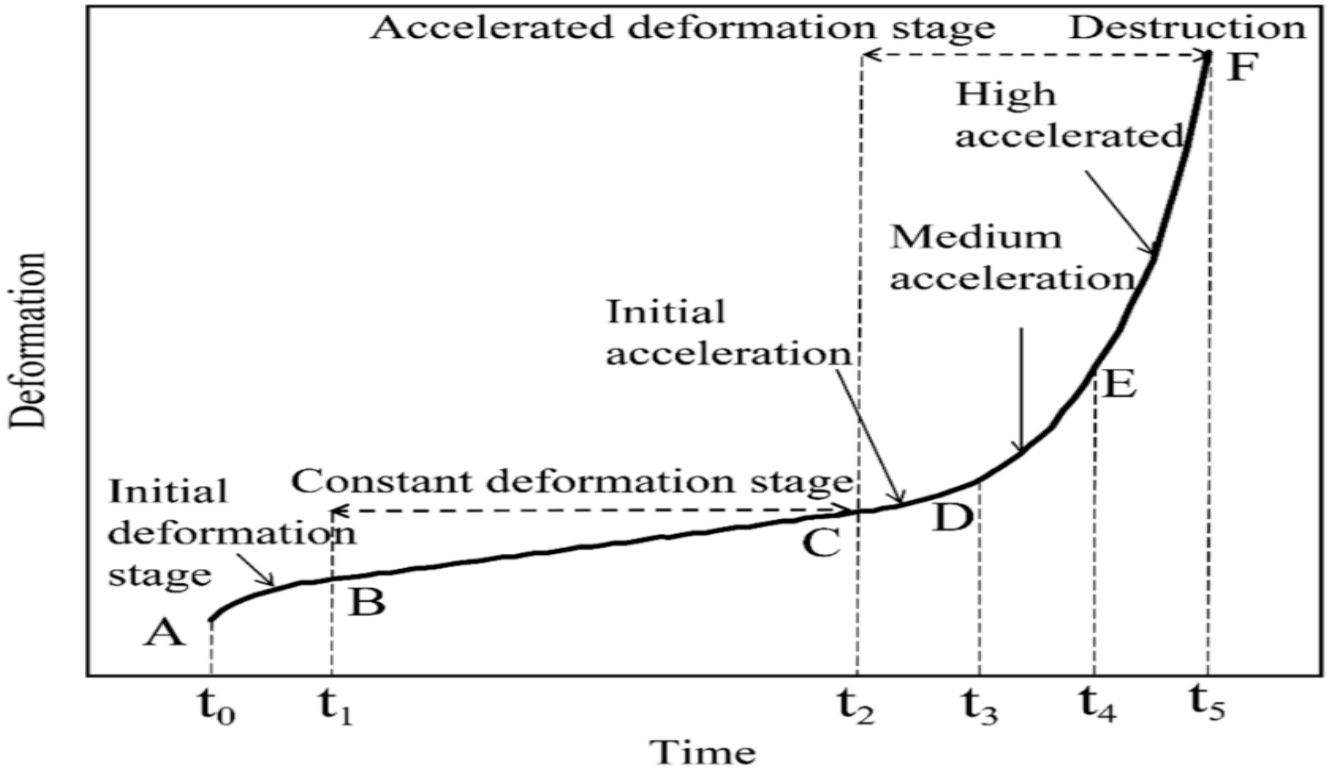


Figure 4: Kinematic stages of slope creep deformation[40]

In geological settings subjected to dynamic disturbances, early warning criteria depend heavily on the accumulation and dissipation of mechanical energy. For earthquake-induced hazards, stability thresholds are dictated by a critical acceleration limit, which is derived directly from the inherent shear strength and frictional resistance of the slope material[2]. When transient peak ground acceleration surpasses this specific threshold, slopes experience rapid non-linear displacement escalation, signaling the onset of co-seismic mass movement[76]. Similarly, in deep underground excavations, warning parameters are established by monitoring the intensity and

ISSN 2278-2540 | DOI: 10.51583/IJLTEMAS | Volume XV, Issue VI, June 2026

spatial concentration of microseismic events. Sudden spikes in the logarithmic energy density or abrupt variations in dominant frequency amplitudes serve as reliable indicators that the rock mass is transitioning from localized stress adjustment to macroscopic shear fracturing[77,78]. Emerging field investigations even suggest that thermodynamic responses can define instability limits. Internal slope temperature variations, specifically anomalous sharp peak and gentle slope fluctuation patterns, strongly correlate with high-intensity rainfall infiltration. These thermal signatures provide an independent physical metric to establish joint thresholds alongside conventional precipitation limits, ultimately enhancing the reliability of predictive alarms before physical detachment occurs[38].

Prediction And Forecasting Models

Statistical and Heuristic Methods

Heuristic techniques, such as the Analytic Hierarchy Process and fuzzy logic, formulate landslide susceptibility by relying entirely on expert judgment to assign relative weights to conditioning parameters[79]. While these knowledge-driven strategies successfully integrate qualitative geomorphological experience, their inherent subjectivity introduces notable inconsistencies and uncertainties into spatial hazard assessments[64,80]. Quantitative statistical models bypass this subjective reliance. They directly analyze the mathematical correlations between historical landslide inventories and underlying topographic or environmental datasets[2,61]. Among bivariate approaches, the Information Value model measures the propensity for slope failure by calculating the logarithmic ratio of landslide density within a specific factor class against the regional average[56,57]. This formulation yields a transparent, physically interpretable index where positive values denote a direct contribution to instability[5,56,81]. The computational simplicity of IV mapping efficiently isolates the individual influence of geo-environmental parameters. It is, however, fundamentally restricted by linear assumptions[5,81]. Because it evaluates each variable independently, the traditional IV approach fails to capture complex, nonlinear interactions among triggering mechanisms, frequently resulting in factor suppression or misrepresentation in highly heterogeneous terrains[80,81]. To resolve missing data anomalies in categories lacking historical failures, researchers occasionally apply a Modified Information Value technique. This mathematically adjusts the discrete calculations to ensure all parameter classes contribute meaningfully to the statistical analysis[80,82]. Extending beyond bivariate limitations, multivariate techniques like logistic regression compute the combined influence of independent continuous and categorical variables on a binary stability outcome[23,83]. LR models estimate the probability of slope failure through a sigmoidal function. They utilize partial regression coefficients to quantify the log-odds ratio of an event occurring under specific site conditions[23,82]. This multivariate capacity allows analysts to identify dominant causative factors without assuming a normal distribution within the input data[23]. To ensure the statistical independence of selected factors before executing logistic regression, researchers must rigorously apply multicollinearity diagnostics, typically identifying and discarding redundant variables through Variance Inflation Factor and tolerance thresholds[23,80,84]. Despite this analytical rigor, logistic regression remains constrained by its foundational assumption of linearity between predictors and the target logit[85]. Consequently, LR formulations often exhibit diminished predictive accuracy when processing highly dimensional, non-linear geospatial relationships[71,85]. Empirical models therefore routinely yield moderate discrimination capacities[63]. To circumvent these mathematical boundaries while preserving interpretability, modern assessments increasingly deploy these traditional statistical outputs not as final susceptibility indices, but as weighted spatial priors that feed directly into advanced ensemble learning architectures[56,81]. Furthermore, the statistical boundaries generated by IV assessments are increasingly repurposed to optimize non-landslide sampling; extracting negative training points exclusively from IV-designated low-susceptibility zones systematically reduces the spatial bias associated with purely random sampling protocols[80,84].

Physically Based Models

Limit equilibrium methods establish the fundamental physical basis for slope stability forecasting by defining the factor of safety as the mathematical ratio of the available shear strength to the downslope driving shear stress[86]. For shallow failures where the rupture depth is significantly smaller than the overall slope length, analysts routinely apply the infinite slope model[19,27]. This formulation assumes that the failure plane develops

ISSN 2278-2540 | DOI: 10.51583/IJLTEMAS | Volume XV, Issue VI, June 2026

strictly parallel to the topographic surface, effectively allowing stability to be evaluated within a rigid, individual slice of soil[27]. Under this geometry, the driving forces are governed by the gravitational weight of the soil mass, which depends directly on the slope angle and the saturated or unsaturated unit weight of the material[27,86]. Conversely, the resisting shear strength is quantified using the Mohr-Coulomb failure criterion, relying on fundamental geotechnical properties including effective cohesion, the angle of internal friction, and prevailing pore water pressures[27]. When evaluating more complex, deep-seated, or non-circular sliding geometries, single-body infinite slope assumptions become inadequate. Researchers instead utilize method of slices techniques, such as the Bishop, Janbu, Spencer, Morgenstern-Price, and Sarma formulations. These approaches partition the potential sliding mass into multiple discrete vertical blocks to satisfy varied combinations of horizontal, vertical, and rotational equilibrium[2]. Operating solely on mechanical equilibrium, these rigid-body analyses are frequently coupled with transient hydrological equations to model rainfall-induced instability. Models including TRIGRS, SHALSTAB, and SINMAP integrate the infinite slope stability equation with physical infiltration models, such as the Green-Ampt approximation or Richards' equation, to capture the subsurface progression of wetting fronts[87]. As meteoric water percolates into the soil matrix, the resultant increase in pore-water pressure and concurrent dissipation of matric suction fundamentally reduce the effective stress acting on the failure plane[27]. This hydrodynamic alteration degrades the available shear resistance, progressively lowering the factor of safety until it drops below unity, marking the theoretical onset of physical failure[86–88]. Despite their computational efficiency, traditional limit equilibrium methods remain constrained by their foundational mathematical assumptions. They treat the geomaterial as a completely rigid body, ignore internal stress-strain constitutive relationships, and compute only an average safety factor across the entire predefined slip surface. These macroscopic averaging obscures localized stress concentrations and prevents the simulation of progressive mechanical yielding. To transcend these analytical limitations, contemporary physical forecasting increasingly relies on advanced stress-strain numerical modeling utilizing finite element or finite difference techniques. These computational environments dispense with predefined slip geometries and explicitly simulate material deformation, strain localization, and stiffness degradation under dynamic loading[2,5]. Within these numerical frameworks, the factor of safety is typically extracted using the shear strength reduction technique[5,89]. This procedure iteratively divides the input cohesion and internal friction angle by a scalar reduction factor until the numerical model fails to reach equilibrium[90]. The threshold reduction value triggers macroscopic slope failure often identified through abrupt nodal displacement or the coalescence of continuous plastic shear zones, is then designated as the system's actual safety factor. By directly linking localized mechanical responses to global stability limits, this reduction methodology bypasses the rigid-body constraints of limit equilibrium analysis and precisely localizes irregular failure surfaces without prior geometric estimation[89,90].

Data-Driven Models

Data-driven prediction techniques bypass the requirement for explicit physical parameters by extracting mathematical correlations directly from historical observations and environmental datasets[3]. Ensemble machine learning algorithms currently dominate regional susceptibility mapping due to their capacity to process high-dimensional, nonlinear geospatial inputs[84,91,92]. Random Forest aggregates multiple decision trees through bootstrap sampling and random feature selection, a mechanism that effectively minimizes variance and controls overfitting[54,80,84]. It readily handles multicollinearity and automatically quantifies variable importance through metrics like Gini impurity[54,84]. Alternatively, gradient boosting frameworks such as XGBoost construct decision trees sequentially to correct the prediction residuals of preceding iterations[54,80]. By incorporating second-order Taylor expansion and explicit regularization terms, XGBoost actively penalizes model complexity[54,56,84]. This ensures high predictive precision even when dealing with severely imbalanced hazard inventories[54,84]. While ensemble techniques require predefined input variables, deep learning architectures automatically extract hierarchical representations directly from raw multi-source data[64,93]. Convolutional neural networks utilize successive convolutional and pooling operations to capture complex spatial dependencies across topographic and geological layers[5,64,86]. Because they reduce dimensionality without significant loss of information, these networks translate pixel-level variations into spatial probabilities of slope failure[6,64,86]. Predicting the precise temporal occurrence of a failure demands distinct sequence modeling capabilities to process non-stationary monitoring streams, such as cumulative displacement or groundwater fluctuations[34,94]. Long short-term memory networks and gated recurrent units overcome the gradient vanishing problems inherent in standard

ISSN 2278-2540 | DOI: 10.51583/IJLTEMAS | Volume XV, Issue VI, June 2026

recurrent neural networks by employing specialized memory blocks and gating mechanisms[34,94]. These structures selectively retain informative historical trends while filtering high-frequency noise, making them highly effective for forecasting progressive step-like displacements and identifying short-term acceleration precursors[5,62,94]. To capture both geometric morphology and dynamic kinematics, contemporary frameworks frequently fuse these distinct neural architectures. Dual-autoencoder systems couple multilayer perceptrons with sequence networks to simultaneously compress static environmental parameters and extract deep evolutionary features from temporal windows[3,93]. More recently, attention-based Transformer models have been deployed to bypass the step-wise information propagation limits of traditional sequential networks. By allocating attention weights globally across an entire time series, Transformers better capture abrupt, impulse-driven responses and long-range dependencies, such as the delayed slope degradation triggered by seismic tail waves[3]. Furthermore, graph neural networks address the spatial autocorrelation assumptions of standard grid-based models by treating monitoring locations as irregular nodes. This approach preserves the non-Euclidean topological relationships of natural terrain, aggregating feature information through spatial connectivity to improve boundary detection and hazard localization in complex orogenic environments[17]. While these advanced neural architectures offer unprecedented capabilities in processing complex spatial topologies, selecting the appropriate predictive framework ultimately requires balancing computational cost, data availability, and the necessity for physical interpretability. To visually summarize these distinct operational pipelines, Figure 5 contrasts the deterministic workflow of physically based models against the multi-source architecture of data-driven frameworks. Furthermore, to synthesize the broader critical trade-offs across all methodologies, Table 2 provides a comprehensive comparison of the statistical, physically based, and data-driven forecasting models currently utilized in geohazard assessments.

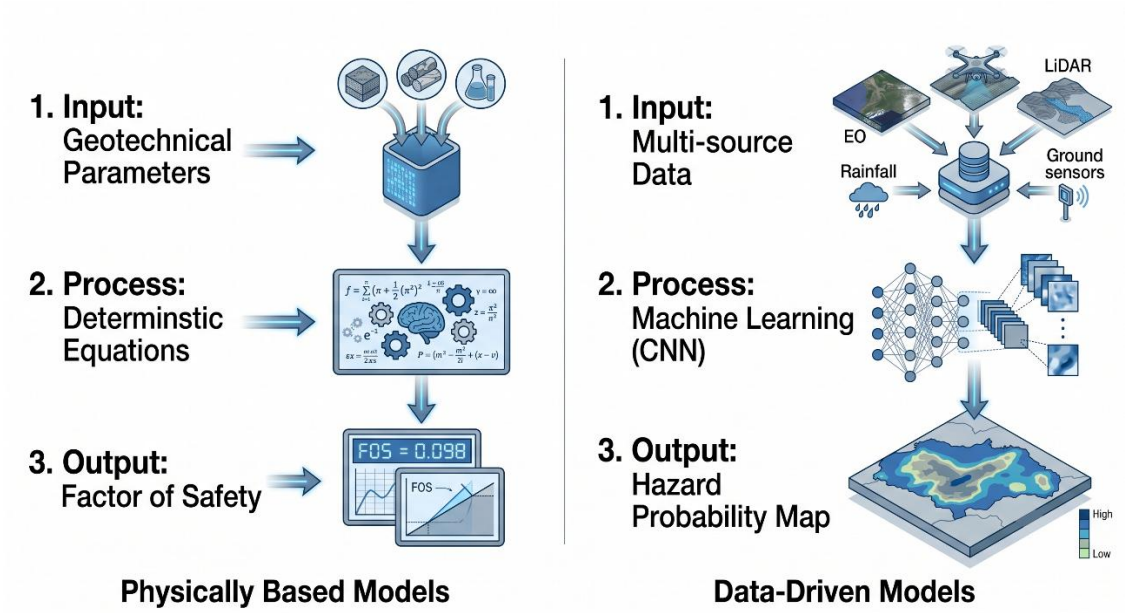


Figure 5: Comparative workflows of physically based vs. data-driven forecasting models

Table 2: Summary of core mechanisms, primary advantages, and major limitations of geological hazard forecasting models

Model Category	Specific Algorithms / Frameworks	Core Mechanism	Primary Advantages	Major Limitations	Source
Heuristic & Statistical	AHP, Information Value (IV), Logistic Regression	Weighs causative conditioning factors via pairwise comparison	Offers high structural transparency, simple mathematical computation,	Relies heavily on subjective expert judgment and lacks the capacity to simulate	[8,80,95]

ISSN 2278-2540 | DOI: 10.51583/IJLTEMAS | Volume XV, Issue VI, June 2026

		matrices or applies relative statistical probability calculations to historical data.	and the direct integration of subjective expert knowledge.	explicit physical failure mechanics.	
Physically Based	Limit Equilibrium, Finite Element, TRIGRS	Models specific transient triggering conditions and calculates safety factors based on topographic and hydrological inputs.	Grounded in explicit physical principles, providing a comprehensive basis for understanding the continuous dynamics of complex hazard chains.	Computationally expensive and demand precise, high-resolution geotechnical and hydrological input parameters to function accurately.	[88]
Ensemble Machine Learning	Random Forest, XGBoost	Aggregates numerous decision trees utilizing parallel bagging or sequential gradient boosting algorithms.	Excels at capturing complex non-linear relationships among environmental variables and quantitatively ranks feature importance.	Operates as an opaque mathematical algorithm that remains highly susceptible to sampling biases and training data imbalances	[55,84,96]
Deep & Sequence Learning	CNNs, LSTMs, Transformers	Employs gated memory cells or multi-head self-attention modules to process variable-length sequential data.	Automatically extracts long-term spatiotemporal dependencies and features from continuous time-series monitoring sequences.	Highly computationally intensive, requiring extensive training datasets and heavy hardware optimization to function effectively.	[62,73,97]

Hazard Prevention and Control

Engineering Interventions

Engineering interventions counteract mass wasting through mechanical resistance and hydrodynamic regulation. Anti-slide piles and retaining walls deliver immediate lateral support by transferring upper sliding forces into stable, deeper bedrock strata. When installed at the over-steepened toe of a slope, these rigid boundaries arrest progressive shear failure and constrain localized bulging[50]. To address internal tensile and shear deficiencies, systematic rock bolting and anchored wire mesh configurations actively bind fractured rock masses together. These reinforcement anchors perform reliably in high-relief seismic zones, although their holding capacity can degrade if prolonged dynamic shaking induces anchor pullout[10]. To overcome the limitations of strictly rigid supports, stabilization design increasingly incorporates yielding or composite structures. Deep underground excavations, for example, utilize energy-absorbing mechanisms such as concrete-filled steel pipes coupled with high-pressure advanced grouting to accommodate substantial geostatic deformations while sealing surrounding fissures against fluid ingress[98]. Similarly, inclined steel grouting pipes injected into loess embankments establish an interconnected cementitious network that densifies the soil matrix and physically impedes capillary moisture migration[49]. Hydrological control remains equally necessary to prevent the accumulation of

ISSN 2278-2540 | DOI: 10.51583/IJLTEMAS | Volume XV, Issue VI, June 2026

destabilizing pore water pressures[10]. Surface interceptor drains and cut-off ditches rapidly channel meteoric runoff away from vulnerable failure scarps, effectively minimizing infiltration and subsequent matric suction loss[50]. Beneath the topographic surface, perforated subsurface pipes and deep drainage galleries systematically relieve elevated groundwater levels, directly mitigating hydraulic fracturing and base heave in soft-ground environments[10,99]. In steep catchments prone to high-velocity debris flows, physical mitigation shifts toward kinetic energy dissipation. Closed-type check dams are strategically positioned along channel convergence points to intercept fluidized solid volumes. Deploying sequential barriers such as an upper dam to immediately attenuate initial flow momentum and a lower terminal dam to trap residual materials, dramatically reduces the destructive velocity reaching downstream infrastructure[29]. For isolated kinematic rockfall events, passive interceptors like flexible catchment nets, earthen bunds, and diversion trenches capture descending blocks[10]. Stepped buffering platforms filled with composite materials can also smoothly dissipate terminal kinetic energy before rocks strike transportation corridors[42]. In shallower unstable terrains, bioengineering interventions frequently supplement structural mechanics. Deep-rooted vegetation physically binds topsoil to resist fluvial scour[10]. Planting live cuttings alongside driven steel nails and natural fiber mats yields a hybrid reinforcement that limits frost heaving and shallow rainfall-induced sliding[100].

Ecological Mitigation Methods

Plant root systems mechanically reinforce unstable slopes by physically binding loose soil particles and increasing the apparent cohesion of the localized terrain[18,19]. This bio-mechanical interaction elevates the overall shear strength of the soil matrix without significantly altering its internal angle of friction. Deep-rooted woody species naturally offer superior anchoring capacity compared to shallow-rooted grasses, as they penetrate deeper soil horizons to interlock with underlying stable strata[10,23]. Beyond physical anchoring, vegetation exerts profound hydrological control over slope dynamics. Canopy structures intercept incoming precipitation and shield the vulnerable surface from direct erosive runoff[18,100]. Below the surface, active root water uptake and evapotranspiration consistently reduce volumetric soil moisture, thereby preserving matric suction and aiding in the rapid desaturation of the soil profile[18,100]. This hydrological reinforcement becomes particularly pronounced during the spring and summer vegetative growing seasons[100]. Root systems nonetheless exhibit a complex dual behavior; while they actively draw down moisture, their physical penetration can simultaneously create preferential flow channels that, under extreme rainfall, might locally accelerate rapid water infiltration and momentarily elevate pore water pressures[19,23]. To systematically harness these biological benefits, practitioners increasingly deploy soil and water bioengineering techniques across degraded or artificially cut terrains. Hydroseeding is frequently applied to steep, bare embankments by spraying a customized slurry containing seeds, nutrients, and sediments, which accelerates the establishment of a stabilizing surface root network. For somewhat deeper structural stabilization, brush layering embeds live cut branches such as salix cuttings, directly into excavated slope terraces to provide immediate mechanical resistance. Because young vegetative cuttings and seeds remain highly vulnerable to rain washout before establishing a mature root architecture, biodegradable geotextiles, primarily coconut fiber mats, are typically anchored over the treated areas to prevent immediate topsoil loss. These biological components are routinely integrated into hybrid stabilization frameworks, such as live crib walls or combined soil-nailing arrays, where the maturing vegetation progressively assumes the primary load-bearing function as the temporary wooden or steel structural elements degrade over subsequent decades. Optimal shear resistance within these systems is achieved by planting a diverse composite of grasses, shrubs, and trees, which generates an overlapping, multi-tiered root matrix[100]. Despite these distinct mechanical and hydrological advantages, the absolute efficacy of bioengineering remains strictly bounded by the physical limits of the rhizosphere. Root reinforcement rarely extends beyond a vertical depth of 0.5 to 2.0 meters, rendering purely vegetative mitigation insufficient against deep-seated kinematic failures dictated by underlying geological structural discontinuities[84]. Because full biological interventions are constrained by the physical limits of the rhizosphere, strong disaster risk reduction frequently demands a hybrid approach. To visually contextualize this integration, Figure 6 illustrates a stabilized slope cross-section, contrasting the shallow soil reinforcement provided by ecological bioengineering against the deep, lateral support required from structural retaining walls.

ISSN 2278-2540 | DOI: 10.51583/IJLTEMAS | Volume XV, Issue VI, June 2026

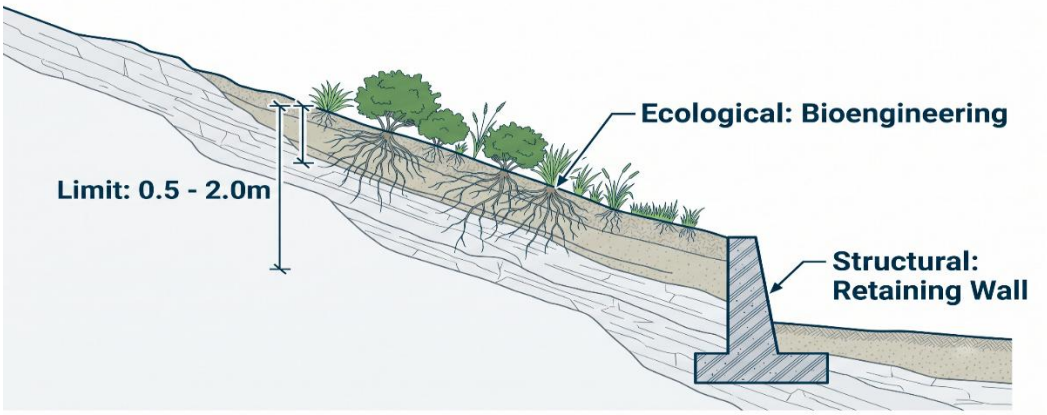


Figure 6: Cross-section of a hybrid mitigation framework illustrating the integration of structural toe support and shallow ecological root reinforcement

Non-Structural Risk Management

Translating spatially explicit susceptibility models into binding land-use regulations represents the primary mechanism for decoupling human exposure from geohazard threats. By integrating predictive hazard maps into regional master plans, municipal authorities can systematically restrict residential and commercial development within high-probability failure zones, thereby preventing the artificial amplification of risk associated with unregulated peri-urban expansion[92,101]. This regulatory approach frequently involves delineating strict no-construction buffer zones along steep, unstable topography or river valleys prone to cascading debris flows[92,102]. In regions already burdened by extensive infrastructure, strategic land-use planning shifts toward managed retreat, subsidizing the proactive relocation of exposed settlements and critical utilities to geologically stable lowlands[85]. However, spatial zoning inherently requires a complementary evaluation of community vulnerability to accurately prioritize these interventions. Quantitative vulnerability assessments achieve this by intersecting physical exposure metrics such as the distribution of building footprints, gross domestic product density, and agricultural acreage with socioeconomic indicators that dictate local coping capacities[95]. Utilizing composite metrics like the Social Development Index or Human Development Index alongside demographic data allows analysts to isolate specific social fragilities[101,102]. These indices frequently reveal that migrant populations and economically marginalized groups, who often reside in informal settlements with inadequate drainage and weak social networks, experience disproportionately high vulnerability to mass movements[102]. Mapping these socioeconomic disparities ensures that hazard mitigation resources are directed toward communities lacking intrinsic adaptive capacity rather than relying strictly on geographic proximity to a hazard[79,101]. Once high-vulnerability clusters are identified, risk managers implement targeted evacuation strategies guided by predictive runout simulations. Delineating the precise spatial trajectory and terminal extent of potential debris flows or rockfalls provides the physical basis for designing safe, accessible evacuation routes and strategically positioning emergency shelters away from anticipated impact corridors[4,92,102]. The effectiveness of these logistical protocols depends entirely on localized preparedness and the integration of community-based early warning systems. Disseminating real-time hazard alerts via telecommunication networks facilitates rapid vertical or horizontal evacuation before extreme rainfall thresholds are breached[25,27,47]. To ensure these alerts translate into immediate action, authorities must sustain ongoing public awareness campaigns, conduct routine community drills, and foster local participation in monitoring efforts, which collectively empower residents to execute orderly evacuations during sudden-onset environmental crises[25,85,102]. While these community-driven protocols represent the final layer of defense, effective disaster risk reduction ultimately relies on the strategic integration of all available countermeasures.

To synthesize this multi-tiered approach, Table 3 categorizes the structural, ecological, and non-structural mitigation strategies discussed throughout this section, highlighting their specific target mechanisms and operational lifespans.

ISSN 2278-2540 | DOI: 10.51583/IJLTEMAS | Volume XV, Issue VI, June 2026

Table 3:Classification of structural, ecological, and non-structural geological hazard mitigation strategies

Mitigation Category	Specific Interventions	Target Mechanism	Operational Lifespan & Function	Source
Structural / Rigid	Anti-slide piles, retaining walls, rigid linings.	Resists sliding forces; transfers localized stress to stable deep bedrock. Directly opposes shear failure.	Immediate lateral support; blocks mass movement. Static, long-term structural stabilization.	[50,99]
Structural / Dynamic	Flexible rock barriers, yielding supports, rock bolts, energy-dissipation platforms.	Absorbs kinetic energy via shape-changing properties. Accommodates large deformations; enhances rock mass cohesion.	Dynamic shock absorption; prevents sudden brittle failure; actively adapts to progressive stress.	[10,42,98]
Hydrological Control	Deep well dewatering, surface drainage ditches, siphon pipelines.	Lowers groundwater table; mitigates pore water pressure surges. Reduces rainfall infiltration.	Continuous seepage control; prevents static liquefaction and hydraulic fracturing.	[50,103,104]
Ecological (Bioengineering)	Live crib walls, hydroseeding, deep-rooted vegetation buffers.	Roots mechanically bind soil particles; increases shear strength. Intercepts rainfall runoff; regulates soil moisture via evapotranspiration.	Self-strengthening long-term stabilization as roots mature; continuous erosion control; ecological restoration.	[18,100]
Non-Structural	Land-use planning, community relocation, early warning systems (EWS), risk zonation.	Reduces human and infrastructure exposure to hazards. Delivers preemptive alerts before catastrophic failure.	Proactive risk avoidance; continuous life-cycle situational awareness; zero physical terrain footprint.	[102,105]

DISCUSSION AND FUTURE PERSPECTIVES

Current Technical Limitations

Ground-based sensor networks frequently experience data loss, signal discontinuities, and physical damage when deployed in harsh operating environments. Extreme weather events, mechanical vibrations, and heavy dust physically degrade instrumentation, while signal obstruction in deep topographical incisions disrupts wireless telemetry[15,62]. These transmission anomalies create missing values that alter time-series structures, directly causing analytical failures in predictive algorithms. While statistical filters are routinely applied to remove such ambient noise, they introduce a secondary operational risk. Rigid statistical boundaries often fail to differentiate between common measurement noise and the abrupt, high-frequency anomaly signals that characterize actual slope destabilization[62]. This means significant precursory indicators are inadvertently discarded before they reach the analytical stage. Macro-scale observation platforms face equally significant environmental barriers that complicate continuous spatial monitoring. Passive optical remote sensing is inherently constrained by its dependence on clear atmospheric conditions, rendering it largely ineffective during monsoon seasons or prolonged cloud cover when hydro-meteorological hazards are most likely to initiate[6,15]. Conversely, active microwave systems bypass cloud interference but remain highly susceptible to geometric and atmospheric distortions. In steep alpine topographies, inherent side-looking radar geometries induce severe foreshortening, layover, and shadowing effects, which physically obscure deformation signals. Even in observable areas, dense vegetation canopies and fluctuating soil moisture cause rapid temporal decorrelation. Atmospheric phase screens generated by tropospheric and ionospheric variations produce spatially coherent phase shifts that artificially mimic true ground displacement[7,57]. The presence of these pervasive environmental artifacts fundamentally

ISSN 2278-2540 | DOI: 10.51583/IJLTEMAS | Volume XV, Issue VI, June 2026

undermines the reliability of contemporary machine learning and deep learning forecasting architectures. Because deep neural networks are highly data-driven, they frequently overfit to site-specific atmospheric or geometric noise, inadvertently learning to classify these artifacts as actual geodetic deformation[7]. This noise sensitivity drives a persistent operational bottleneck: algorithms optimized to maximize detection hit rates frequently generate unacceptable volumes of false alarms. Such false positive alerts overwhelm manual verification capacities and ultimately erode the social credibility of early warning systems during long-term operation[6]. This issue is compounded by severe domain shift, where predictive models trained on specific lithologies, sensor wavelengths, or temporal sampling intervals experience drastic performance degradation when transferred to novel geographic regions or different satellite platforms[7]. Resolving these false alarm rates necessitates the fusion of multi-source heterogeneous datasets, yet integrating disparate geological, meteorological, and kinematic streams introduces profound scaling challenges. Different sensor platforms operate across incompatible spatial resolutions, temporal frequencies, and data formats, leading to semantic inconsistency and information loss during analytical integration. Predictive models typically discretize continuous geological bodies into rigid grid cells, which mathematically homogenizes localized subsurface properties. This scale-induced simplification obscures the spatial continuity of deep structural planes and weak interlayers that actually govern failure mechanics. Consequently, the resulting algorithms function predominantly as opaque black boxes that map statistical correlations rather than underlying physical processes. The absence of transparent, physically grounded reasoning in these models severely limits their engineering applicability, as decision-makers cannot readily interpret the causal mechanisms driving the automated hazard alerts[6].

Future Research Directions

Future algorithmic architectures are progressively integrating physical laws directly into machine learning pipelines to resolve the inherent opacity and data dependency of pure data-driven forecasting. Physics-informed neural networks embed partial differential equations and geomechanical constraints such as elastic dislocation or poroelastic adjustment, directly into the loss function of the model[7,106]. By penalizing predictions that violate fundamental principles like mass conservation or kinematic consistency, these hybrid approaches force the neural network to output physically plausible deformation trajectories, even when trained on sparse or noisy datasets[6]. This regularization strategy is highly effective at mitigating the influence of atmospheric phase screens and temporal decorrelation in satellite interferometry, which frequently cause standard deep learning models to learn environmental artifacts as actual ground displacement[7]. While the theoretical advantages of physics-informed artificial intelligence are substantial, applying these coupled models across highly heterogeneous lithologies remains computationally expensive and mathematically challenging because idealized governing equations rarely match the discontinuous reality of natural rock masses[6]. To overcome these computational barriers, researchers propose integrating adaptive sampling, active learning, and physics-guided surrogate models to maintain high predictive accuracy while minimizing sample demand and runtime[6,107]. Parallel to these algorithmic developments, the physical monitoring landscape is transitioning toward the implementation of digital twin technologies. Virtual replicas of physical infrastructure and geological environments fuse real-time Internet of Things sensor streams—including groundwater piezometers, microseismic geophones, and distributed fiber optics—with three-dimensional geological models and Building Information Modeling systems. This continuous data assimilation allows analysts to simulate subsurface stress redistributions and fluid migrations dynamically, effectively replacing static regional susceptibility maps with interactive, time-resolved virtual testing environments. Integrating these digital replicas with edge computing architectures further reduces transmission latency by enabling localized anomaly detection and immediate decision-making at the sensor node before data is relayed to centralized cloud servers. Beyond predicting isolated slope failures, future hazard assessments must explicitly quantify the complex dynamics of cascading multi-hazard disaster chains[27,95]. Extreme meteorological forcing or seismic shocks frequently initiate primary instabilities, such as massive rockfalls, which rapidly fluidize into debris flows, dam adjacent river channels, and ultimately trigger catastrophic outburst floods[53,108]. Because traditional models generally evaluate these phenomena independently, they severely underestimate the compounded spatial exposure, kinetic energy amplification, and secondary environmental contamination generated during a continuous disaster sequence[1,95]. To capture these cascading interactions, emerging theoretical frameworks propose generalized geological-environmental hazard

ISSN 2278-2540 | DOI: 10.51583/IJLTEMAS | Volume XV, Issue VI, June 2026

chain effect matrices that iteratively calculate the overlapping spatial and temporal probabilities of primary mass movements and their secondary impacts[1]. Translating these conceptual matrices into operational tools requires coupled numerical simulations, such as combined discrete element and shallow-water equation solvers, that can explicitly track the transfer of momentum, progressive material entrainment, and rheological transformations across the entire hazard cascade. To ensure these advanced modeling chains can be deployed across diverse geographic domains without suffering severe performance degradation, ongoing research is increasingly experimenting with self-supervised foundation models. By pre-training neural architectures on massive, unlabeled, multi-modal Earth observation datasets, these foundation models extract highly generalized spatiotemporal representations that can be transferred to new topographies or climatic zones with minimal local fine-tuning[6,7].

CONCLUSION

The management of geological hazards currently occupies a transitional space between reactive post-disaster evaluation and proactive, real-time assessment. As infrastructure increasingly permeates volatile terrain, the necessity of understanding the intricate physical fields driving these failures has never been more urgent. Hazards do not emerge from isolated triggers. They evolve through complex hydro-mechanical and tectonic interactions that dynamically degrade material stability. Technological interventions have significantly enhanced our ability to track these destructive processes. We now integrate orbital synthetic aperture radar, aerial point clouds, and distributed wireless sensor networks to construct continuous, high-resolution surveillance systems. Concurrently, predictive analytics has transitioned from rigid heuristic equations to advanced data-driven algorithms. Deep learning architectures successfully digest vast, high-dimensional datasets. They allow researchers to isolate spatial anomalies and morphological patterns with unprecedented speed. Despite these observational and computational achievements, significant bottlenecks obstruct the realization of intelligent forecasting systems. Environmental artifacts profoundly limit data acquisition. Atmospheric noise and severe terrain distortions regularly compromise remote sensing fidelity. More fundamentally, prevailing artificial intelligence models operate predominantly as opaque systems. They map mathematical correlations instead of underlying physical mechanisms. This structural opacity makes them highly vulnerable to domain shifts and environmental interference, frequently resulting in unacceptable false alarm rates that undermine early warning networks. Furthermore, existing evaluations often treat susceptibility as a static baseline, failing to accommodate the cascading nature of complex disaster sequences. To transcend these limitations, the next generation of hazard management must actively bridge the persistent divide between macroscopic statistics and localized geomechanics. Incorporating partial differential equations directly into machine learning pipelines offers a promising pathway. This forces computational outputs into physically plausible trajectories. Scaling these hybrid systems alongside interactive digital twins will effectively transition regional static maps into dynamic virtual testing environments. Ultimately, coupling physically grounded predictive architectures with self-supervised foundation models will empower engineers to simulate and mitigate evolving multi-hazard disaster chains globally.

REFERENCES

1. Zhang, S., Song, J., Zhan, L., Xu, Q., Zhang, L., & Chen, Y. (2025). Geological-environmental hazard chain: Phenomena, process, and principle. In Science China Earth Sciences (Vol. 68, Number 10, pp. 3085–3107). Science China Press. https://doi.org/10.1007/s11430-024-1602-x
2. Gupta, K., Satyam, N., Falak, & Rahim, S. (2026). Mapping Co-seismic Landslide Susceptibility: An Overview of Current and Emerging Methods. Indian Geotechnical Journal. https://doi.org/10.1007/s40098-026-01495-5
3. Zhang, X., Huang, S., & Gao, B. (2026). Full-waveform CNN–transformer neural network for regional coseismic landslide susceptibility modeling: A case study of the 2022 Luding earthquake, China. Engineering Geology, 362. https://doi.org/10.1016/j.enggeo.2025.108520
4. Wang, H., Sun, P., Mao, J., Wang, T., & Li, K. (2026). Dynamic-process-based quantitative hazard assessment for earthquake-induced landslide clusters in the Northern Mountain of Tianshui. Landslides. https://doi.org/10.1007/s10346-026-02776-z

ISSN 2278-2540 | DOI: 10.51583/IJLTEMAS | Volume XV, Issue VI, June 2026

5. Huang, Y., Xu, C., Shao, X., He, X., Xiao, Z., Xu, X., Xie, Y., Nie, X., & Li, X. (2026). Landslide assessment research in the three gorges reservoir area: A review of methodological advances and future directions. In Bulletin of Engineering Geology and the Environment (Vol. 85, Number 2). Springer Science and Business Media Deutschland GmbH. https://doi.org/10.1007/s10064-025-04733-x
6. Zhou, M., Mei, G., Ma, Z., Xu, N., & Peng, J. (2026). AI for geosafety: motivations, advances, challenges, and opportunities. In Bulletin of Engineering Geology and the Environment (Vol. 85, Number 5). Springer Science and Business Media Deutschland GmbH. https://doi.org/10.1007/s10064-026-04961-9
7. Alonso-Díaz, A., Fontes, M., Teixeira, A. C., Wdowinski, S., & Sousa, J. J. (2026). Multi-Temporal InSAR and Machine Learning for Geohazard Monitoring: A Systematic Review with Emphasis on Noise Mitigation and Model Transferability. In Remote Sensing (Vol. 18, Number 9). Multidisciplinary Digital Publishing Institute (MDPI). https://doi.org/10.3390/rs18091356
8. Okegbola, M. O., Owolabi, O., Sheng, Z., & Liu, Y. (2026). Integrating Multi-Temporal LiDAR and AHP for Landslide Detection and Susceptibility Mapping in Prince George's County, Maryland. Journal of Safety Science and Resilience, 100311. https://doi.org/10.1016/j.jnlssr.2026.100311
9. Naskar, D. C. (2026). Advances in Engineering Geophysics: Concepts and Applications (Vol. 9). Springer Nature Switzerland. https://doi.org/10.1007/978-3-032-28000-8
10. Eze, K. N., Ilesanmi, O. O., Igah, G. C., Abidola, A. Q., Ojefia, F. E., & Adekoya, A. M. (2025). Seismic rockfall risk assessments and mitigation strategies for transportation infrastructure in high-risk regions. Discover Geoscience, 3(1). https://doi.org/10.1007/s44288-025-00182-x
11. Yao, X., Huang, M., Shi, F., & Yu, L. (2025). Intelligent and Sustainable Classification of Tunnel Water and Mud Inrush Hazards with Zero Misjudgment of Major Hazards: Integrating Large-Scale Models and Multi-Strategy Data Enhancement. Sustainability (Switzerland), 17(24). https://doi.org/10.3390/su172411286
12. Xing, K., Li, S., Dou, J., Chen, F., Wang, L., Dong, A., Daud, H., & Zhang, L. (2026). Integrating multi-geometry InSAR and explainable machine learning for mapping potential landslide areas in reservoir regions. Remote Sensing of Environment, 341. https://doi.org/10.1016/j.rse.2026.115442
13. Ma, T., Duan, Y., Duan, W., Wang, H., Tang, C., Wang, K., & Cheng, G. (2025). Research on Intelligent Early Warning System and Cloud Platform for Rockburst Monitoring. Applied Sciences (Switzerland), 15(20). https://doi.org/10.3390/app152011098
14. Kuang, Z., Li, S., Qiu, S., Huang, Y., & Chang, S. (2026). Identifying zones of rockburst-collapse compound hazards in deep tunnels. Journal of Rock Mechanics and Geotechnical Engineering. https://doi.org/10.1016/j.jrmge.2026.03.019
15. Zhang, Y., Sun, Y., Yan, Y., Wang, S., & Ge, L. (2026). Research Status, Challenges and Future Perspectives of Geological Hazard Monitoring Methods in Mining Areas. In Remote Sensing (Vol. 18, Number 9). Multidisciplinary Digital Publishing Institute (MDPI). https://doi.org/10.3390/rs18091333
16. Zhang, X., Duan, X., Khalil, U., Muhammadi, M. A., Elmannai, H., Algarni, A. D., & Kucher, D. E. (2026). Multi-sensor deep learning approach for landslide susceptibility mapping under climate and anthropogenic pressures. Physics and Chemistry of the Earth, 143. https://doi.org/10.1016/j.pce.2026.104305
17. Goli Mokhtari, L. (2026). Optimizing graph neural networks for rockfall susceptibility mapping: a feature selection and hazard prediction approach. Natural Hazards, 122(1). https://doi.org/10.1007/s11069-025-07855-3
18. Ehsan, M., Anees, M. T., Bakar, A. F. B. A., & Ahmed, A. (2025). A review of geological and triggering factors influencing landslide susceptibility: artificial intelligence-based trends in mapping and prediction. In International Journal of Environmental Science and Technology (Vol. 22, Number 16, pp. 17347–17382). Springer Nature. https://doi.org/10.1007/s13762-025-06741-6

ISSN 2278-2540 | DOI: 10.51583/IJLTEMAS | Volume XV, Issue VI, June 2026

19. Liao, Z., Wu, J., Deng, Z., Lü, Q., & Yu, Y. (2026). Tectonic and microtopographic controls on aspect-dependent distribution of rainfall-induced shallow landslides. Geomorphology, 511, 110416. https://doi.org/10.1016/j.geomorph.2026.110416
20. Li, Y., Yang, H., Zheng, L., Qi, W., Chongyi, E., & Gao, T. (2026). Formation mechanism and stability assessment of the Attabad landslide-dammed lake along the China-Pakistan Karakoram Highway using remote sensing technology. Landslides. https://doi.org/10.1007/s10346-026-02697-x
21. Zhang, J. W., Xu, W. Z., Song, Z. X., Zhang, Y., Yang, J. N., Dong, X. K., Wu, S. K., Bai, X. Y., Zhang, S. L., & Li, X. (2026). An overview of coal-rock-gas compound dynamic disasters in China and the structural classification of risk-prone areas. In Journal of Central South University (Vol. 33, Number 3, pp. 997–1027). Central South University. https://doi.org/10.1007/s11771-026-6221-6
22. Shi, W., Chen, G., Meng, X., Bian, S., Jin, J., Wu, J., Huang, F., & Chong, Y. (2023). Formation and Hazard Analysis of Landslide Damming Based on Multi-Source Remote Sensing Data. Remote Sensing, 15(19). https://doi.org/10.3390/rs15194691
23. Bukhari, S. N. U. H., Ahmed, K. S., Ikram, N., Usmani, N. A., Sadiq, S., & Gardezi, S. A. H. (2026). Post-earthquake landslide hazard evolution: Spatio-temporal analysis of active fault zone in Western Himalayas. Journal of Mountain Science, 23(5), 2088–2110. https://doi.org/10.1007/s11629-025-0204-1
24. Ran, S., Zhou, W., Weng, Y., Chi, F., Wang, D., Cao, X., & Ma, G. (2026). Causative environment-informed active landslide detection with InSAR monitoring: Empowering reservoir slope hazard management. International Journal of Applied Earth Observation and Geoinformation, 146. https://doi.org/10.1016/j.jag.2025.105079
25. Malik, B. A., & Koner, R. (2024). Comprehensive review of the monitoring and sensing system in slopes with a special focus on the mining sector. In Environmental Science and Pollution Research (Vol. 31, Number 59, pp. 66588–66614). Springer. https://doi.org/10.1007/s11356-024-35693-6
26. Nan, K., Luo, Y., Xu, Q., Zhao, B., & Song, H. (2025). Reactivation mechanisms of the ancient Dahekou landslide in Hanzhong City, Shaanxi Province, China. Journal of Mountain Science, 22(4), 1245–1260. https://doi.org/10.1007/s11629-024-9130-x
27. Dolojan, N. L. J., Takahashi, T., Hashimoto, M., Shibayama, A., Nomura, R., Terada, K., & Moriguchi, S. (2025). Integrated multihazard study combining qualitative and quantitative analyses of floods, landslides, and debris flows: A case study on the impacts of Typhoon Yun-Yeung on Iwaki City, Fukushima. International Journal of Disaster Risk Reduction, 127. https://doi.org/10.1016/j.ijdrr.2025.105647
28. Moradi, S., Heinze, T., Budler, J., Gunatilake, T., Kemna, A., & Huisman, J. A. (2021). Combining site characterization, monitoring and hydromechanical modeling for assessing slope stability. Land, 10(4). https://doi.org/10.3390/land10040423
29. Lee, D. H., Lee, S. R., & Park, J. Y. (2025). Coupled modeling framework for proactive design of debris-flow barrier placements. Scientific Reports, 15(1). https://doi.org/10.1038/s41598-025-15290-4
30. You, Q., Wang, F., Ma, H., Fu, Z., & Feng, Y. (2026). Lithological controls on clustered landslides: a case study of landslides triggered by Typhoon Gaemi (2024) in Zixing, Hunan Province, China. Landslides. https://doi.org/10.1007/s10346-026-02762-5
31. Wang, J. H., & Xu, W. J. (2025). Slope stability and failure dynamics of rainfall-induced landslide: Algorithm and applications. Computers and Geotechnics, 177. https://doi.org/10.1016/j.compgeo.2024.106919
32. Zhang, L., Wang, Y., & Liu, J. (2024). Mechanical interpretation of retrogressive failure in mild dip rock slopes induced by slope cutting and rainfall: a case study in Yunnan, China. Bulletin of Engineering Geology and the Environment, 83(1). https://doi.org/10.1007/s10064-023-03503-x
33. Li, K., Sun, P., Wang, H., & Ren, J. (2024). Insight into failure mechanisms of rainfall induced mudstone landslide controlled by structural planes: From laboratory experiments. Engineering Geology, 343. https://doi.org/10.1016/j.enggeo.2024.107774

ISSN 2278-2540 | DOI: 10.51583/IJLTEMAS | Volume XV, Issue VI, June 2026

34. Li, Y., Hu, X., Zhang, H., Zheng, H., & Li, N. (2025). Displacement prediction and failure mechanism analysis of rainfall-induced colluvial landslides. Journal of Hydrology, 660. https://doi.org/10.1016/j.jhydrol.2025.133361
35. Fusco, F., Bordoni, M., Tufano, R., Vivaldi, V., Meisina, C., Valentino, R., Bittelli, M., & De Vita, P. (2022). Hydrological regimes in different slope environments and implications on rainfall thresholds triggering shallow landslides. Natural Hazards, 114(1), 907–939. https://doi.org/10.1007/s11069-022-05417-5
36. Du, H., Wan, Y., Wang, D., Cao, B., & Liu, G. (2025). Research on deformation characteristics and mechanisms of an open pit coal mine landslide event in extremely cold region. Scientific Reports, 15(1). https://doi.org/10.1038/s41598-025-27509-5
37. An, H., & Ouyang, C. (2026). From sky to ground: A multi-source observations-physical model cascade for debris flow forecasting in inaccessible alpine regions. Engineering Geology, 369. https://doi.org/10.1016/j.enggeo.2026.108810
38. Li, Z., Chen, J. P., Cao, C., Zhang, W., Xu, P., Zheng, L. J., Jing, Y., & Hu, J. Y. (2025). Temperature and deformation response under the influence of continuous typhoons in seasonal permafrost rainfall-induced landslide evolution. Natural Hazards, 121(11), 13093–13116. https://doi.org/10.1007/s11069-025-07312-1
39. Weng, M. C., Chao, W. A., Yang, C. M., Teo, T. A., Li, K. W., & Hsiao, Y. T. (2026). Assessing earthquake-induced displacements of large-scale landslide by in-situ monitoring and discrete element analysis. Engineering Geology, 368. https://doi.org/10.1016/j.enggeo.2026.108775
40. Minghui, M., Hongsheng, M., Ningfei, L., Dong, S., Liang, Q., Mingli, L., Xu, Z., & Wulin, M. (2025). The research on the evolution characteristics of multi-geneses Dashui gully high-locality landslide in the upper reaches of Minjiang river. Bulletin of Engineering Geology and the Environment, 84(7). https://doi.org/10.1007/s10064-025-04389-7
41. He, N., Qu, X., Yang, Z., Xu, L., & Gurkalo, F. (2023). Disaster Mechanism and Evolution Characteristics of Landslide–Debris-Flow Geohazard Chain Due to Strong Earthquake—A Case Study of Niumian Gully. Water (Switzerland), 15(6). https://doi.org/10.3390/w15061218
42. Zhao, X., Fen, W., Dai, Z., Jiao, W., Geng, J., Xiong, Q., & Zhang, N. (2026). Dynamic rockfall risk assessment using multi-source data fusion and 3D simulation: a case study of Jiaohua rock. Scientific Reports, 16(1). https://doi.org/10.1038/s41598-026-36769-8
43. Zhang, M., Xing, A., Li, K., Zhuang, Y., Chang, W., & Liu, Y. (2023). Debris flows in Lebai gully along the Yarlung Tsangpo River in Tibet: characterization, causes, and dynamic prediction of potential debris flows. Environmental Earth Sciences, 82(1). https://doi.org/10.1007/s12665-022-10694-1
44. Wang, F., Ren, Q., Wu, K., & Zheng, C. (2025). Formation and Evolutionary Mechanisms of Slope Instability Disasters at Exposed Surfaces of Deep-Large Collapse Pit Induced by Underground Mining Activities. Indian Geotechnical Journal. https://doi.org/10.1007/s40098-025-01319-y
45. Xia, K., Chen, C., Zheng, Y., Zhang, H., Liu, X., Deng, Y., & Yang, K. (2019). Engineering geology and ground collapse mechanism in the Chengchao Iron-ore Mine in China. Engineering Geology, 249, 129–147. https://doi.org/10.1016/j.enggeo.2018.12.028
46. Yang, Y., Li, J., Shi, W., Yang, C., & Yan, L. (2024). Numerical Investigation of Failure Characteristics and Debris Movement in the Madaling Landslide Using Coupled FDM–DEM. Geotechnical and Geological Engineering, 42(4), 2745–2765. https://doi.org/10.1007/s10706-023-02703-2
47. Zeng, T., Jin, B., Liu, Y., Glade, T., Wang, F., Yin, K., & Peduto, D. (2024). Cut slope hazard analysis and management based on a double-index precipitation threshold: a case study in the Miaoyuan area (Eastern China). Environmental Earth Sciences, 83(24). https://doi.org/10.1007/s12665-024-11987-3
48. Yang, F., & Hasan, M. (2026). Comprehensive risk mapping and management of rainfall-induced slope failures in urbanizing subtropical regions. Scientific Reports, 16(1). https://doi.org/10.1038/s41598-026-49114-w

ISSN 2278-2540 | DOI: 10.51583/IJLTEMAS | Volume XV, Issue VI, June 2026

49. Fan, J., Zhang, Y., Peng, Y., Xing, Z., Yuan, K., Cui, J., Liu, B., & Zhou, W. (2025). Study on the disaster mechanism and prevention technology of embankment slip-collapse after extreme rainfall in the loess area. Scientific Reports, 15(1). https://doi.org/10.1038/s41598-025-04920-6
50. Guo, J., Meng, F., & Guo, J. (2024). Gradual Failure of a Rainfall-Induced Creep-Type Landslide and an Application of Improved Integrated Monitoring System: A Case Study. Sensors, 24(22). https://doi.org/10.3390/s24227409
51. Fei, P., Yi, Q., Deng, M., Wang, B., Song, Y., & Liu, L. (2025). Study on the Deformation Mechanism of Shallow Soil Landslides Under the Coupled Effects of Crack Development, Road Loading, and Rainfall. Water (Switzerland), 17(8). https://doi.org/10.3390/w17081196
52. Zhao, W., Cong, P., Ma, X., Yi, M., Liu, C., Gao, J., & Zhang, Y. (2026). Landslide Hazard Identification and Prediction in Complex Mountainous Areas Using Ascending and Descending Orbits InSAR Technology. Sensors, 26(8). https://doi.org/10.3390/s26082455
53. Yu, Z., Zhan, J., Yao, Z., & Peng, J. (2024). Characteristics and mechanism of a catastrophic landslide-debris flow disaster chain triggered by extreme rainfall in Shaanxi, China. Natural Hazards, 120(8), 7597–7626. https://doi.org/10.1007/s11069-024-06518-z
54. Zhao, F., Hu, B., Wu, H., Li, W., Zhang, C., Hei, L., Wang, L., Wu, W., & Yang, L. (2026). Landslide susceptibility assessment based on a frequency ratio-ensemble learning framework and InSAR constraints. Advances in Space Research. https://doi.org/10.1016/j.asr.2026.05.039
55. Guan, X., Chen, P., Liu, H., Li, Z., Qiu, L., Zhu, C., Hong, Y., Yao, Y., & Li, Z. (2026). Dynamic landslide susceptibility assessment in Zhouqu County, China, based on SBAS-InSAR and a Stacking ensemble learning model. Advances in Space Research. https://doi.org/10.1016/j.asr.2026.04.081
56. Zhou, H., Lu, M., Liu, F., Jiang, K., & Wang, Y. (2026). Landslide Hazard InSAR Monitoring and Stability Evaluation Method for Large Open-Pit Mines: A Case Study of the Baiyinhua Open-Pit Mine, China. Processes, 14(12), 1844. https://doi.org/10.3390/pr14121844
57. Cheng, X., Zeng, B., Tang, L., Yuan, J., Ai, D., & Huang, W. (2026). Multi-model landslide integrated hazard detection using SBAS-InSAR and U-Net segmentation. Bulletin of Engineering Geology and the Environment, 85(3). https://doi.org/10.1007/s10064-026-04780-y
58. Yang, A., Wang, Y., Yin, K., Gui, L., Liu, X., Liu, Y., Li, X., & Zhao, B. (2026). Progressive deformation and post-failure residual displacement of the 16 October 2025 Tongren loess landslide, Qinghai, China: insights for long-term extra-high voltage transmission line monitoring. Landslides. https://doi.org/10.1007/s10346-026-02786-x
59. Guo, Z., Zeng, T., Zhang, Y., Yu, W., Wang, L., Guo, Z., & Glade, T. (2025). A novel hybrid model integrating high resolution remote sensing and stacking ensemble techniques for landslide susceptibility mapping: Application to event-based landslide inventory. Geomorphology, 486. https://doi.org/10.1016/j.geomorph.2025.109886
60. Ahmadi, P., Valadan Zoej, M. J., Mokhtarzade, M., Kardan, N., Ahmadi, P., & Ghaderpour, E. (2026). TLE-FEDformer: A Frequency-Domain Transformer Framework for Multi-Sensor Multi-Temporal Flood Inundation Mapping. Remote Sensing, 18(6). https://doi.org/10.3390/rs18060895
61. Gurung, B., Chen, N., Hu, G., Khadka, N., Sapkota, L., Gouli, M. R., & Tian, S. (2026). Integrating machine learning and numerical methods for enhanced landslide susceptibility and hazard mapping in the Bhotekoshi watershed, central Nepal. Journal of Mountain Science. https://doi.org/10.1007/s11629-025-9951-2
62. Dong, X., Li, S., Ma, R., Tian, W., Zhao, K., Xiang, H., Zhu, J., & Qiu, Y. (2025). Cloud-based slope risk monitoring and early warning system for open-pit coal mines: a case study of Zhonglian Runshi. Scientific Reports, 15(1). https://doi.org/10.1038/s41598-025-28190-4
63. Pornbunyanon, T., Jitpat, P., & Suwanno, P. (2026). Rainfall-conditioned landslide susceptibility mapping using an FR–CART hybrid framework in southern Thailand. Progress in Disaster Science, 29. https://doi.org/10.1016/j.pdisas.2026.100530
64. Rezaie, F., Eghbali, M., Panahi, M., Shafapourtehrany, M., Batur, M., Moeini, H., Özener, H., & Kalantari, Z. (2025). Advanced deep learning–based approaches for semantic segmentation in precise landslide detection and susceptibility assessment. Ecological Informatics, 92. https://doi.org/10.1016/j.ecoinf.2025.103447

ISSN 2278-2540 | DOI: 10.51583/IJLTEMAS | Volume XV, Issue VI, June 2026

65. Kulkarni, S., Jasani, S., Kulkarni, S., & Wadmare, J. (2025). Datasets, Features, and Advanced Techniques in Landslide Susceptibility Prediction: a Review. In SN Computer Science (Vol. 6, Number 7). Springer. https://doi.org/10.1007/s42979-025-04395-2
66. Luo, W., Zheng, J., Miao, Y., & Gao, L. (2024). Raspberry Pi-Based IoT System for Grouting Void Detection in Tunnel Construction. Buildings, 14(11). https://doi.org/10.3390/buildings14113349
67. Cacciuttolo, C., Atencio, E., Komarizadehasl, S., & Lozano-Galant, J. A. (2024). Internet of Things Long-Range-Wide-Area-Network-Based Wireless Sensors Network for Underground Mine Monitoring: Planning an Efficient, Safe, and Sustainable Labor Environment. In Sensors (Vol. 24, Number 21). Multidisciplinary Digital Publishing Institute (MDPI). https://doi.org/10.3390/s24216971
68. Kondo, A., & Matsushi, Y. (2026). Mechanisms of rainfall-induced shallow landslides regulated by hydrological subsurface structures: Cases in granite and granodiorite areas in Northern Abukuma Mountains, Japan. Engineering Geology, 366. https://doi.org/10.1016/j.enggeo.2026.108692
69. Pei, X. (2022). Design of a Wireless Sensor Network-Based Risk Assessment Algorithm for Cave Collapse. Mobile Information Systems, 2022. https://doi.org/10.1155/2022/8568181
70. Su, G., Huang, J., Jiang, J., Niu, W., & Liu, Z. (2026). Real-time microseismic monitoring and intelligent early warning of collapse in the shallow-buried tunnel in relatively fractured hard rocks. Engineering Failure Analysis, 185. https://doi.org/10.1016/j.engfailanal.2025.110364
71. Ramya, H. N., & Nagesh, M. A. (2026). Advanced generative adversarial network for rainfall-induced landslide hazard mapping. Journal of the Brazilian Society of Mechanical Sciences and Engineering, 48(4). https://doi.org/10.1007/s40430-025-06288-0
72. Wu, P., Yang, L., Li, W., Huang, J., & Xu, Y. (2023). Construction Safety Risk Assessment and Early Warning of Nearshore Tunnel Based on BIM Technology. Journal of Marine Science and Engineering, 11(10). https://doi.org/10.3390/jmse11101996
73. Li, W., Li, Y., Zhao, Y., & Xu, D. (2025). Optimization of monitoring and early warning technology for mine water disasters using microservices and long short-term memory algorithm. Journal of Supercomputing, 81(4). https://doi.org/10.1007/s11227-025-07033-z
74. Satyaningsih, R., Jetten, V., Ettema, J., Sopaheluwakan, A., Lombardo, L., & Nuryanto, D. E. (2023). Dynamic rainfall thresholds for landslide early warning in Progo Catchment, Java, Indonesia. Natural Hazards, 119(3), 2133–2158. https://doi.org/10.1007/s11069-023-06208-2
75. Feng, B., Zeng, P., Li, T., Sun, X., Zhu, X., Fan, X., & Xu, Q. (2025). Acceleration stage detection and dynamic model selection for real-time landslide time-of-failure predictions. Acta Geotechnica. https://doi.org/10.1007/s11440-025-02878-3
76. Pitilakis, K., Fotopoulou, S., Manakou, M., Karafagka, S., Petridis, C., Pitilakis, D., & Raptakis, D. (2024). Towards seismic risk reduction of critical facilities combining earthquake early warning and structural monitoring: a demonstration study. Bulletin of Earthquake Engineering, 22(14), 6893–6927. https://doi.org/10.1007/s10518-024-02046-0
77. Wang, C., Guo, M., Ji, Z., Gong, Y., Lu, C., Qi, P., Zhu, K., Zhu, C., Gao, M., & Chen, X. (2026). Degradation-buckling-shear mechanism of earthquake-induced bedding rock landslides in the Three-rivers basin: Insights from field investigation and shaking table test. Engineering Geology, 367. https://doi.org/10.1016/j.enggeo.2026.108722
78. Kuang, Z., Qiu, S., Li, S., Xiao, Y., Feng, G., Huang, Y., & Chang, S. (2025). A new early warning method for rockbursts and compound rockburst–collapse hazards in deeply-buried tunnels based on energy density. Tunnelling and Underground Space Technology, 164. https://doi.org/10.1016/j.tust.2025.106828
79. Sharma, A., Sajjad, H., Roshani, & Rahaman, M. H. (2024). A systematic review for assessing the impact of climate change on landslides: research gaps and directions for future research. In Spatial Information Research (Vol. 32, Number 2, pp. 165–185). Springer Science and Business Media B.V. https://doi.org/10.1007/s41324-023-00551-z
80. Abdelkader, M. M., Daoud, A. M. A., Abdel-Gawad, A. G., & Csámer, Á. (2025). Improving landslide susceptibility mapping: The role of non-landslide sample selection in machine learning

ISSN 2278-2540 | DOI: 10.51583/IJLTEMAS | Volume XV, Issue VI, June 2026

models. Remote Sensing Applications: Society and Environment, 40. https://doi.org/10.1016/j.rsase.2025.101759

81. Wang, L., Wang, X., Zhang, H., Xu, Y., Chen, Q., Wu, J., Wu, W., & Ma, D. (2026). Regional landslide susceptibility assessment via coupled modeling and sample optimization: A case study of Dujiangyan, China. Journal of Hydrology: Regional Studies, 66. https://doi.org/10.1016/j.ejrh.2026.103570
82. Zhang, Y., Yang, Z., Liu, J., Zeng, Y., Sun, Y., & Tan, J. (2026). Vulnerability of mountain road networks to rainfall-induced landslide hazards. Journal of Mountain Science, 23(1), 188–202. https://doi.org/10.1007/s11629-025-9673-5
83. Singh, G., Kumar, S., Karmakar, R., & Mishra, A. K. (2025). Rapid assessment of landslide exposure to elements at risk for decision support in regional landslide forecasting. Discover Geoscience, 3(1). https://doi.org/10.1007/s44288-025-00299-z
84. Joshi, B. R., Bhandary, N. P., Acharya, I. P., Niraj, K. C., & Bhandari, C. (2026). Integration of information value with machine learning method for an enhanced predictive performance in landslide susceptibility mapping. Discover Geoscience, 4(1), 152. https://doi.org/10.1007/s44288-026-00517-2
85. Shen, L., Zhao, X., Liu, H., Sheng, H., Chi, Z., & Zhang, C. (2026). Enhancing landslide susceptibility mapping analysis through neighborhood feature aggregation and interpretable machine learning: Implications for disaster prevention in valley-type urban planning. Journal of Environmental Management, 402. https://doi.org/10.1016/j.jenvman.2026.129117
86. Nguyen, H. H. D., Song, C. H., & Kim, Y. T. (2025). Semi-quantitative risk assessment: From rainfall-induced landslides to the risk of persons in buildings. Bulletin of Engineering Geology and the Environment, 84(9). https://doi.org/10.1007/s10064-025-04420-x
87. Dolojan, N. L. J., Moriguchi, S., Hashimoto, M., & Terada, K. (2021). Mapping method of rainfall-induced landslide hazards by infiltration and slope stability analysis: A case study in Marumori, Miyagi, Japan, during the October 2019 Typhoon Hagibis. Landslides, 18(6), 2039–2057. https://doi.org/10.1007/s10346-020-01617-x
88. Musaib, A., Aparna, V., & Divya, P. V. (2026). Integrating TRIGRS and RAMMS for the spatiotemporal prediction of rainfall induced landslides and landslide trajectory: a case study. Natural Hazards, 122(3). https://doi.org/10.1007/s11069-025-07779-y
89. Chavali, R. V. P., Bayati, Z., Tremblay, A., Saeidi, A., Lévesque, Y., & Lambert, M. (2026). Integrated Remote Sensing and Slope Stability Modeling for Back Analysis of Sensitive Clay Landslides. Geotechnical and Geological Engineering, 44(2). https://doi.org/10.1007/s10706-026-03628-2
90. Meng, G., Li, H., Wu, B., Liu, G., Ye, H., & Zuo, Y. (2023). Prediction of the Tunnel Collapse Probability Using SVR-Based Monte Carlo Simulation: A Case Study. Sustainability (Switzerland), 15(9). https://doi.org/10.3390/su15097098
91. Sahin, E. K., Demir, S., Ozturk, M., & Duzce, M. S. (2025). Geoscience in the era of generative artificial intelligence (Geo[AI]-LSM): understanding the potential benefits of Google Gemini in producing landslide susceptibility mapping. Advances in Space Research. https://doi.org/10.1016/j.asr.2025.11.048
92. Utthasini, M., Ilampooranan, I., Singh, S. K., Kanga, S., Kumar, P., Halder, K., Pradhan, B., Srivastava, A. K., Chatterjee, R. S., Chakrabortty, R., Ali, T., & Meraj, G. (2026). Enhancing landslide susceptibility mapping in the Himalayas: geospatial and machine learning with explainable AI (XAI). Gondwana Research, 149, 262–290. https://doi.org/10.1016/j.gr.2025.08.003
93. Ou, L., Zhang, Y., & Chen, Y. (2026). Intelligent Triggering of Safety Risk Warning in Metro Tunnel Construction: A Two-Stage Framework Integrating Static and Dynamic Data. Buildings, 16(8). https://doi.org/10.3390/buildings16081550
94. Peng, Y., Li, Q., Wang, H., Liu, Z., & Xia, Y. (2026). Automated TBM tunnel-face collapse detection system based on spatiotemporal fusion and attention mechanism with muck characteristics and operational data. Tunnelling and Underground Space Technology, 174. https://doi.org/10.1016/j.tust.2026.107688

ISSN 2278-2540 | DOI: 10.51583/IJLTEMAS | Volume XV, Issue VI, June 2026

95. Yang, X., Yan, Y., Zhou, X., Zhu, L., Ma, M., Zhang, J., Chen, Y., & Gao, L. (2025). Risk of Compound Typhoon Disaster Chains: Insights from Southeastern China. International Journal of Disaster Risk Science, 16(5), 870–887. https://doi.org/10.1007/s13753-025-00674-x
96. Sarna, S., Gutierrez, M., Mooney, M., & Zhu, M. (2022). Predicting Upcoming Collapse Incidents During Tunneling in Rocks with Continuation Length Based on Influence Zone. Rock Mechanics and Rock Engineering, 55(10), 5905–5931. https://doi.org/10.1007/s00603-022-02971-z
97. Liu, H., Ma, T., Lin, Y., Peng, K., Hu, X., Xie, S., & Luo, K. (2024). Deep Learning in Rockburst Intensity Level Prediction: Performance Evaluation and Comparison of the NGO-CNN-BiGRU-Attention Model. Applied Sciences (Switzerland), 14(13). https://doi.org/10.3390/app14135719
98. Yu, X., Zhang, X., Feng, X. T., Wang, F., Shi, M., Yang, C., Luo, H., Yang, Y., & Wang, Y. (2026). Fracture evolution and differential mechanical response of surrounding rock in deep tunnel excavation: A case study under complex geological conditions. Engineering Geology, 362. https://doi.org/10.1016/j.enggeo.2025.108534
99. Calvi, A. (n.d.). Tunnels Collapses: Case Studies and Key Failure Mechanisms.
100. Capobianco, V., Palau, R. M., Solheim, A., Gisnås, K., Gilbert, G., Danielsson, P., & van der Keur, P. (2024). The potential use of nature-based solutions as natural hazard mitigation measure for linear infrastructure in the Nordic Countries. In Geoenvironmental Disasters (Vol. 11, Number 1). Springer Science and Business Media Deutschland GmbH. https://doi.org/10.1186/s40677-024-00287-4
101. Mondragón-Rodríguez, A., & Quesada-Román, A. (2026). Integrating geomorphological and socio-spatial factors for landslide risk zonation in Atenas, Costa Rica. Discover Hazards, 2(1), 8. https://doi.org/10.1007/s44475-026-00012-9
102. Jain, S. K., Jain, S. K., & Ahmad, R. (2025). Glacial lake outburst floods (GLOFs): causes, modeling, and mitigation in Indian Himalayan region. GeoJournal , 90(2). https://doi.org/10.1007/s10708-025-11326-4
103. Gong, Z., Fu, X., & Cheng, X. (2026). Excavation Stability of Tunnel Structure in Water-Rich Areas. Applied Sciences, 16(2), 902. https://doi.org/10.3390/app16020902
104. Nguyen, H. S., Khau, T. L., & Huynh, T. T. (2025). Investigation of Natural and Human-Induced Landslides in Red Basaltic Soils. Water (Switzerland), 17(9). https://doi.org/10.3390/w17091320
105. He, X., Xu, C., Huang, Y., Yang, Q., Wang, W., & Xiao, Z. (2026). Evolution of Geological Hazard Prevention in the Three Gorges Reservoir Area: Insights from Planning and Implementation. Earthquake Research Advances, 100464. https://doi.org/10.1016/j.eqrea.2026.100464
106. Ling, Q., Chen, W., Zhang, Q., Wang, L., Qu, W., Shu, B., Ren, J., Guo, Q., Qu, J., Li, W., Yang, C., Chen, Y., & Sha, J. (2026). A PINN-based hybrid model with APIDr for interpretable and cross-scenario landslide displacement prediction. Journal of Hydrology, 674. https://doi.org/10.1016/j.jhydrol.2026.135493
107. Xu, L., Zhanping, S., Xiaole, S., Lianbaichao, L., Tong, W., & Shengyuan, F. (2026). Damage quantification and response surface prediction of blasting-induced slope stability based on DFN. Bulletin of Engineering Geology and the Environment, 85(1). https://doi.org/10.1007/s10064-025-04723-z
108. Li, Y., Zhang, C., & Zhang, G. (2025). The development characteristics and formation modes of rainstorm-triggered flash flood disasters in the Hengduan Mountains. Journal of Geographical Sciences, 35(3), 619–640. https://doi.org/10.1007/s11442-025-2337-0